Structure of charmed baryons studied by pionic decays

Hideko Nagahiro,[1,2] Shigehiro Yasui,[3] Atsushi Hosaka,[2,4] Makoto Oka,[3,5] and Hiroyuki Noumi[2]

[1] *Department of Physics, Nara Women's University, Nara 630-8506, Japan*
[2] *Research Center for Nuclear Physics (RCNP), Osaka University, Ibaraki, Osaka 567-0047, Japan*
[3] *Department of Physics, Tokyo Institute of Technology, Meguro 152-8551, Japan*
[4] *J-PARC Branch, KEK Theory Center, KEK, Tokai, Ibaraki 319-1106, Japan*
[5] *Advanced Science Research Center, Japan Atomic Energy Agency, Tokai, Ibaraki, 319-1195, Japan*

(Dated: September 6, 2016)

We investigate the decays of the charmed baryons aiming at the systematic understanding of hadron internal structures based on the quark model by paying attention to heavy quark symmetry. We evaluate the decay widths from the one pion emission for the known excited states, $\Lambda_c^*(2595)$, $\Lambda_c^*(2625)$, $\Lambda_c^*(2765)$, $\Lambda_c^*(2880)$ and $\Lambda_c^*(2940)$, as well as for the ground states $\Sigma_c(2455)$ and $\Sigma_c^*(2520)$. The decay properties of the lower excited charmed baryons are well explained, and several important predictions for higher excited baryons are given. We find that the axial-vector type coupling of the pion to the light quarks is essential, which is expected from chiral symmetry, to reproduce the decay widths especially of the low lying Λ_c^* baryons. We emphasize the importance of the branching ratios of $\Gamma(\Sigma_c^*\pi)/\Gamma(\Sigma_c\pi)$ for the study of the nature of higher excited Λ_c^* baryons.

PACS numbers: 14.20.Lq, 13.30.Eg, 12.39.Jh

arXiv:1609.01085v1 [hep-ph] 5 Sep 2016

I. INTRODUCTION

Understanding of the internal structure of hadrons is an important subject in hadron physics. One of the most important problems is to identify the effective degrees of freedom which should play essential roles at low energies, because the bare quarks do not appear at such a scale due to the color confinement of QCD. To identify the effective degrees of freedom should serve not only for the understanding of the QCD vacuum properties, but also be useful to explain and predict experimental data with simple physical terms. In this respect, what we are aiming at is to establish the economized effective degrees of freedom for various phenomena of the strong interaction physics [1, 2].

The charmed baryons, containing a single heavy charm quark, is a good place to study the hadron structure. One of the important features is the spin symmetry of the heavy quark. QCD predicts that the spin-dependent interaction of the heavy quark is suppressed by $1/m_Q$ and thus in the infinite m_Q limit, the heavy quark spin is decoupled from the dynamics of the light quarks. The dynamical decoupling of the light quark spin and the heavy quark spin is the heavy quark symmetry (HQS) [3].

In the heavy quark limit, the light quark component is called the *brown muck* as the colorful object conserving its total spin [4]. In terms of QCD, the brown muck contains not only light quarks but also light antiquarks as well as gluons. For the spin of the brown muck j, the heavy hadrons are classified to one state with the total spin $J = 1/2$ for $j = 0$ and two degenerate states with the total spin $J = j \pm 1/2$ for $j \geq 1/2$. The former is called the HQS singlet, and the latter is called the HQS doublet. The classification based on the HQS is useful for the investigation of the heavy hadrons, because the brown muck spin serves as an additional conserved quantum number reflecting the internal structure of the heavy hadrons. The HQS appears in many properties of heavy hadrons, such as the mass spectrum and the decay branching ratios[1].

There is another interesting feature of the charmed baryons. In the quark model description, we have two different orbital motions in the low energy excitations. One is the relative motion between two light quarks, so-called ρ-mode. The other is the one between the center-of-mass of the two light quarks and the charm quark, so-called λ-mode. Owing to the mass difference of the light and heavy quarks, the excitation energies of the λ- and ρ-modes are kinematically well separated, and the internal excitations are dominated exclusively by either ρ-mode or λ-mode with only small mixing [23]. This contrasts with light quark baryons where the two modes generally mix largely, and thus is the reason that we can study the two basic modes exclusively in the heavy baryons.

In general, internal structures of hadron are reflected not only in mass spectrum but also in various transition properties such as productions and decays. Among them, two-body decay processes through the one-pion emission are particularly interesting due to the following reasons: (i) The pion couples only to the light quarks, and the charm quark behaves simply as a spectator. The dynamics of the pion is governed by chiral symmetry in a unique manner. Therefore, the transitions accompanying pion emission should bring important information about the dynamics of the two light quarks in a heavy baryon. This is also helpful to understand diquark properties in a heavy baryon. (ii) Some low-lying states of excited charmed baryons have significantly smaller ex-

[1] The heavy quark symmetry can be applied also to exotic heavy hadrons such as hadronic molecules [5–15] as well as to the heavy hadrons in nuclear medium [15–21]. See Ref. [22] as a review for the latter.

citation energies than light baryon excitations, and the emitted pion carries only a small momentum. Therefore, the pion emission from the excited charmed baryons is a good place to study the quark-pion interaction, which should be well determined by the low energy chiral dynamics. This can be checked by comparing the theoretical results with the observed decays of the low-lying charmed baryons.

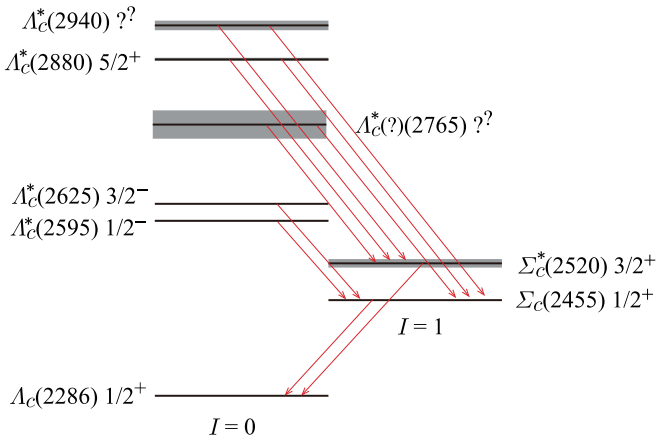

FIG. 1. (color online) Level structure of the charmed baryons with isospin $I = 0$ and $I = 1$ $Y_c(mass)J^P$ considered in this study. The hatched squares denote their total decay widths in Particle Data Group (PDG) [24]. The arrows indicate the possible decay paths with one-pion emission evaluated in this study.

In this paper we consider the pion emission decays from the orbitaly excited charmed baryons [2] $\Lambda_c^*(2595)$, $\Lambda_c^*(2625)$, $\Lambda_c^*(2765)$, $\Lambda_c^*(2880)$, $\Lambda_c^*(2940)$ into $\Sigma_c(2455)\pi$ and $\Sigma_c^*(2520)\pi$, and those from orbital ground state charmed baryons $\Sigma_c(2455)$ and $\Sigma_c^*(2520)$ into $\Lambda_c(2286)\pi$. The decay paths are summarized in Fig. 1. To estimate the decay widths numerically, we employ a non-relativistic constituent quark model with a harmonic oscillator potential as the quark confinement force. The model is rather simple but we expect that essential and universal features can be extracted.

There are previous works investigating strong decays of charmed baryons [3, 18, 25–31]. In Ref. [30], based on heavy hadron chiral perturbation theory the importance of heavy quark symmetry are discussed in the heavy quark limit. In Ref. [18], including the correction terms from the next-to-leading order $\mathcal{O}(1/m_Q)$, relationships between decay widths in several decay channels were obtained. In Ref. [31], non-relativistic quark model calculations were performed and decays of various quark model states were investigated. In the present study, we will also employ the non-relativistic quark model. It is worthwhile to emphasize the difference between the works in Ref. [31] and ours. In Ref. [31], the baryon wave functions are constructed in the so-called LS coupling scheme, while we do in the jj coupling scheme where the brown muck total j is first formed. In doing so, we will derive various relations and selection rules in relation to HQS.

In our study, we will shed light upon the following issues. Firstly, we check the validity of the present framework by calculating the decay widths of the two Σ_c baryons, $\Sigma_c(2455)(J^P = 1/2^+)$ and $\Sigma_c^*(2520)(J^P = 3/2^+)$, which are the orbital ground state of charmed baryons. These baryons decay into $\Lambda_c(2286)\pi$ as the only possible channel in strong decay. Because both the initial and final charmed baryon states are in the orbital ground states in the quark model, those charmed baryons are good objects for confirmation of the validity of our formalism for the one-pion emission. We will see that our results are in reasonably good agreement with the experimental values.

Secondly, we investigate the decay properties of the $\Lambda_c^*(2595)(J^P = 1/2^-)$ and $\Lambda_c^*(2620)(J^P = 3/2^-)$ as the lowest-lying orbital excitations in p-wave. They are interesting because they have the subcomponent, the spin-0 diquark system, which is moving in the p-wave orbital of the λ-mode [27, 32, 33]. They have been observed in e^+e^- collisions and $p\bar{p}$ collisions [34–36] as well as in photoproductions [37]. An interesting feature of them is that the $\Lambda_c^*(2595)(1/2^-)$ baryon has a considerably large decay width into $\Sigma_c\pi$ channel although its phase space is very small. In contrast, $\Lambda_c^*(2625)(3/2^-)$ has a very small width although there is sufficiently large phase space in its decay channel $\Sigma_c\pi$. We show that the quark model description with the λ-mode can explain these decay properties very well for these low-lying Y_c states. We find that, to achieve the good agreements, the πqq interaction Lagrangian of the derivative coupling (axial-vector coupling) is needed to reproduce the experimental decay width. This strongly implies that the non-linear chiral dynamics works for the pion and constituent quarks. We will present that especially decay properties of $\Lambda_c^*(2595)$ are much affected by the isospin breaking effect near the thresholds.

Thirdly, we study higher excited charmed baryons, $\Lambda_c^*(2765)$, $\Lambda_c^*(2880)$ and $\Lambda_c^*(2940)$. Because their spins and parities are not fully determined experimentally, we consider various patterns of assignments of $1/2^\pm$, $3/2^\pm$ and $5/2^\pm$ which are formed by the quark model. By comparing the resulting decay widths with existing experimental data, we will see that several assignments of spin and parity will be excluded.

Finally, we will pay special attention to $\Lambda_c^*(2880)$ for the determination of its spin and parity. In PDG [24], the spin of the $\Lambda_c^*(2880)$ is 5/2 which is determined by the angular distribution of $\Sigma_c(2455)\pi$ decay [24, 38], and the positive parity is inferred from the agreement of the observed decay branching ratio $\Sigma_c^*(2520)/\Sigma_c(2455)$ in comparison with the prediction from heavy quark symmetry [3, 30, 38]. As carefully argued in Ref. [30], how-

[2] In this article, we express the ground and excited charmed baryons as Y_c and Y_c^*.

ever, possible p-wave contribution was simply ignored in the evaluation of the branching ratio. We show that the many configurations for the Λ_c^* baryons with $J^P = 5/2^+$ are turned out to be incompatible with the present experimental data [38] if the p-wave contribution is properly considered. We find that only one configuration leads to the result consistent with the data where p-wave contribution vanishes due to the selection rule working for the pion emission between diquarks, the occurrence of which is a unique feature of heavy baryons where a heavy quark behaves as a spectator, namely in heavy quark symmetry.

This article is organized as follows. In Sec. II, we explain wave functions of the charmed baryons employed in our constituent quark model. In Sec. III we present the formalism for the one-pion emission decay of the charmed baryon. We show our numerical results for the decay widths in Sec. IV. Finally, Sec. V is devoted to the summery.

II. BARYON WAVE FUNCTIONS WITHIN THE QUARK MODEL

We construct the baryon wave functions in a scheme inspired by the heavy quark symmetry. Namely, first we construct a brown muck wave function using light degrees of freedom, which is then combined with the heavy quark to form the total baryon wave functions. In this manner, we will be able to see in a transparent manner various relations and selection rules which are valid in the heavy quark limit. Let us start with the harmonic oscillator Hamiltonian for the orbital wave function,

$$H = -\sum_{i=1}^{3} \frac{\vec{\nabla}_i^2}{2m_i} + \sum_{i\neq j} \frac{k}{2}(\vec{r}_i - \vec{r}_j)^2, \tag{1}$$

where $\vec{r}_i$ are the spatial coordinates of the i-th quark of mass m_i and k the spring constant.

Quark-1 and quark-2 denote the two light quarks of mass m ($m_1 = m_2 = m$), and quark-3 the charm quark of mass M, ($m_3 = M$). The Hamiltonian can be divided into one for the center-of-mass motion $\vec{X}$ and those for the relative motions $\vec{\rho}$ and $\vec{\lambda}$ as

$$H = H_G + H_\rho + H_\lambda, \tag{2}$$

where

$$H_G = -\frac{\vec{\nabla}_X^2}{2(2m+M)} \ , \tag{3a}$$

$$H_\rho = -\frac{\vec{\nabla}_\rho^2}{2m_\rho} + \frac{m_\rho \omega_\rho^2}{2}\vec{\rho}^{\,2} \ , \tag{3b}$$

$$H_\lambda = -\frac{\vec{\nabla}_\lambda^2}{2m_\lambda} + \frac{m_\lambda \omega_\lambda^2}{2}\vec{\lambda}^{\,2} \ . \tag{3c}$$

Here, the coordinate of the center-of-mass $\vec{X}$ is defined as

$$\vec{X} = \frac{1}{2m+M}(m(\vec{r}_1 + \vec{r}_2) + M\vec{r}_3), \tag{4}$$

and $\vec{\rho}$ and $\vec{\lambda}$ are the Jacobi coordinates defined as

$$\vec{\rho} = \vec{r}_1 - \vec{r}_2, \tag{5a}$$

$$\vec{\lambda} = \frac{1}{2}(\vec{r}_1 + \vec{r}_2) - \vec{r}_3. \tag{5b}$$

As indicated in Fig. 2, $\vec{\rho}$ is the relative coordinate between the two light quarks (quark-1 and quark-2), and $\vec{\lambda}$ is the relative coordinate between the center-of-mass of the two light quarks and the charm quark.

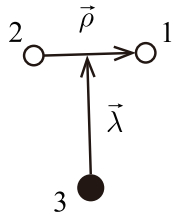

FIG. 2. Difinitions of the Jacobi coordinates $\vec{\rho}$ and $\vec{\lambda}$. The quarks 1 and 2 are the light quarks, and 3 the heavy (charm) quark.

The reduced masses m_λ and m_ρ are defined by

$$m_\rho = \frac{m}{2}, \quad m_\lambda = \frac{2mM}{2m+M}, \tag{6}$$

and the frequencies of the oscillator for λ- and ρ-modes are by

$$\omega_\rho = \sqrt{\frac{3k}{m}}, \quad \omega_\lambda = \sqrt{\frac{k(2m+M)}{mM}}. \tag{7}$$

Orbital wave functions of the three-quark state are expressed by a simple product of the eigenfunctions of the separated Hamiltonians

$$\Psi(\vec{r}_1, \vec{r}_2, \vec{r}_3) = \psi_\lambda(\vec{\lambda})\psi_\rho(\vec{\rho})e^{i\vec{P}\cdot\vec{X}} \ , \tag{8}$$

where $\vec{P}$ is the total momentum of the three-quark state, and $\psi_\lambda(\vec{\lambda})$ and $\psi_\rho(\vec{\rho})$ the wave functions of the Jacobi coordinates $\vec{\lambda}$ and $\vec{\rho}$. The wave functions of the harmonic oscillator are given by

$$\psi_{n\ell m}(\vec{x}) = R_{n\ell}(r)Y_{\ell m}(\hat{x}) \ , \tag{9}$$

where the radial function $R_{n\ell}(r)$ is summarized in Appendix and $Y_{\ell m}$ is the spherical harmonics. We will call the excitation with either $n_\lambda \neq 0$ (radial excitation) or $\ell_\lambda \neq 0$ (orbital excitation) the λ-mode. This is also the case for the ρ-mode. When both λ-mode and ρ-mode happen, this is called the $\lambda\rho$-mode.

The full wave functions of baryons are constructed by products of isospin (flavor) part, spin part, and the orbital part. For the isospin part, we introduce the notation $D^I_{(I_z)}$ for the two light quarks as

$$D^0 : \left\{ D^0_0 = \frac{1}{\sqrt{2}}(ud - du) \right\} \ , \tag{10}$$

for $I = 0$ state, and

$$D^1 : \left\{ D^1_1 = uu, \quad D^1_0 = \frac{1}{\sqrt{2}}(ud - du), \quad D^1_{-1} = dd \right\}, \tag{11}$$

for $I = 1$ states. The flavor wave function of the Λ_c baryons having $I = 0$ is then expressed by $D^0 c$ (c stands for the charm quark), and that of the Σ_c baryons with $I = 1$ is by $D^1 c$.

Similarly, the spin wave functions of the two light quarks are expressed by $d^s_{(s_z)}$,

$$d^0 : \left\{ d^0_0 = \frac{1}{\sqrt{2}}(\uparrow\downarrow - \downarrow\uparrow) \right\} , \tag{12}$$

$$d^1 : \left\{ d^1_1 = \uparrow\uparrow,\ d^1_0 = \frac{1}{\sqrt{2}}(\uparrow\downarrow + \downarrow\uparrow),\ d^1_{-1} = \downarrow\downarrow \right\} . \tag{13}$$

For the charm quark spin, we use the symbol χ_c for either spin up or down.

By making use of these expressions, the full wave functions of the $\Lambda_c(J)$ and $\Sigma_c(J)$ with total spin J are constructed as

$$\Lambda_c(JM) = \left[[\psi_{n_\lambda \ell_\lambda m_\lambda}(\vec{\lambda}) \psi_{n_\rho \ell_\rho m_\rho}(\vec{\rho}), d]^j, \chi_c \right]^J_M D^0 c \ , \tag{14}$$

$$\Sigma_c(JM) = \left[[\psi_{n_\lambda \ell_\lambda m_\lambda}(\vec{\lambda}) \psi_{n_\rho \ell_\rho m_\rho}(\vec{\rho}), d]^j, \chi_c \right]^J_M D^1 c \ , \tag{15}$$

by anti-symmetrizing the light quark part including the color part which is not explicitly shown here. The total spin J of the charmed baryon is given by the sum of the spin of charm quark and the "total" angular momentum j of all the remaining part (so-called *brown muck* [4]) which is obtained by composing the orbital angular momenta ℓ_λ and ℓ_ρ and diquark spin d. For example, the wave functions of orbital ground state for the charmed baryons are given by

$$\Lambda_c(1/2^+) = \left[[\psi_{0s}(\vec{\lambda}) \psi_{0s}(\vec{\rho}), d^0]^0, \chi_c \right]^{1/2} D^0 c \ , \tag{16}$$

$$\Sigma_c(1/2^+) = \left[[\psi_{0s}(\vec{\lambda}) \psi_{0s}(\vec{\rho}), d^1]^1, \chi_c \right]^{1/2} D^1 c \ , \tag{17}$$

and

$$\Sigma^*_c(3/2^+) = \left[[\psi_{0s}(\vec{\lambda}) \psi_{0s}(\vec{\rho}), d^1]^1, \chi_c \right]^{3/2} D^1 c \ . \tag{18}$$

In Table I, we summarize the quark configurations for the charmed baryons considered in this article. The observed Λ_c excited states $\Lambda^*_c(2595)$ and $\Lambda^*_c(2625)$ baryons are, due to their small excitation energies, assigned to be the p-wave excitations of the λ-mode ($n_\lambda = 0$, $\ell_\lambda = 1$) with spin-0 diquark (d^0). Their quark configurations are given by

$$\Lambda^*_c(1/2^-; \lambda\text{-mode}) = \left[[\psi_{0p}(\vec{\lambda}) \psi_{0s}(\vec{\rho}), d^0]^1, \chi_c \right]^{1/2} D^0 c \ , \tag{19}$$

TABLE I. Quark configurations considered in this article. $(n_{\lambda(\rho)}, \ell_{\lambda(\rho)})$ are the nodal and the angular momentum quantum numbers for the $\lambda(\rho)$ motion wave function. The spin wave function of the two light quarks is expressed by d. The brown muck spin and the parity is expressed by j^P. The total angular momentum $\vec{\ell} = \vec{\ell}_\lambda + \vec{\ell}_\rho$ are also shown for $\lambda\rho$-mode. The spin and party J^P and supposed physical charmed baryons are also shown.

Ground states charmed baryons

$(n_\lambda, \ell_\lambda)$	(n_ρ, ℓ_ρ)	d^s	j^P	J^P	possible assignment
$(0,0)$	$(0,0)$	d^0	0^+	$1/2^+$	$\Lambda_c(2286)$
$(0,0)$	$(0,0)$	d^1	1^+	$(1/2,3/2)^+$	$\Sigma_c(2455)$, $\Sigma^*_c(2520)$

Negative parity excited charmed baryons

$(n_\lambda, \ell_\lambda)$	(n_ρ, ℓ_ρ)	d^s	j^P	J^P	possible assignment
$(0,1)$	$(0,0)$	d^0	1^-	$(1/2,3/2)^-$	$\Lambda^*_c(2595)$, $\Lambda^*_c(2625)$
$(0,0)$	$(0,1)$	d^1	0^-	$1/2^-$	
			1^-	$(1/2,3/2)^-$	
			2^-	$(3/2,5/2)^-$	$\Lambda^*_c(2880)(?)$

Positive parity excited charmed baryons

$(n_\lambda, \ell_\lambda)$	(n_ρ, ℓ_ρ)	d^s	j^P	J^P	possible assignment
$(1,0)$	$(0,0)$	d^0	0^+	$1/2^+$	
$(0,2)$	$(0,0)$	d^0	2^+	$(3/2,5/2)^+$	$\Lambda^*_c(2880)(?)$
$(0,0)$	$(1,0)$	d^0	0^+	$1/2^+$	
$(0,0)$	$(0,2)$	d^0	2^+	$(3/2,5/2)^+$	$\Lambda^*_c(2880)(?)$

Positive parity excited charmed baryons ($\lambda\rho$-mode)

$(n_\lambda, \ell_\lambda)$	(n_ρ, ℓ_ρ)	d^s	ℓ	j^P	J^P	possible assignment
$(0,1)$	$(0,1)$	d^1	0	1^+	$(1/2,3/2)^+$	
			1	0^+	$1/2^+$	
				1^+	$(1/2,3/2)^+$	
				2^+	$(3/2,5/2)^+$	$\Lambda^*_c(2880)(?)$
			2	1^+	$(1/2,3/2)^+$	
				2^+	$(3/2,5/2)^+$	$\Lambda^*_c(2880)(?)$
				3^+	$(5/2,7/2)^+$	$\Lambda^*_c(2880)(?)$

and

$$\Lambda^*_c(3/2^-; \lambda\text{-mode}) = \left[[\psi_{0p}(\vec{\lambda}) \psi_{0s}(\vec{\rho}), d^0]^1, \chi_c \right]^{3/2} D^0 c \ . \tag{20}$$

Another possibility to construct the negative parity excited states for Λ^*_c is the so-called ρ-mode excitation ($n_\rho = 0$, $\ell_\rho = 1$), which must have the spin-1 diquark (d^1) due to the anti-symmetrization of the wave function. The total spin j of the brown muck can be $j = 0$, 1 and 2, leading to a HQS singlet with the baryon spin $J = 1/2$, and two HQS doublets $J = (1/2, 3/2)$ and $J = (3/2, 5/2)$, respectively. For example, the concrete

form for the HQS singlet is given by

$$\Lambda_c^*(J^-;\rho\text{-mode}) = \Big[[\psi_{0s}(\vec{\lambda})\psi_{0p}(\vec{\rho}),d^1]^j,\chi_c\Big]^{J=j\pm1/2} D^0 c\ . \tag{21}$$

The minimal configuration for $J^P = 1/2^+$ state for Λ_c baryons is an orbital excitation for the nodal quantum number $n_\lambda = 1$ or $n_\rho = 1$ as with spin-0 diquark given by

$$\Lambda_c^*(1/2^+;n_\lambda{=}1) = \Big[[\psi_{1s}(\vec{\lambda})\psi_{0s}(\vec{\rho}),d^0]^0,\chi_c\Big]^{1/2}. \tag{22}$$

$$\Lambda_c^*(1/2^+;n_\rho{=}1) = \Big[[\psi_{0s}(\vec{\lambda})\psi_{1s}(\vec{\rho}),d^0]^0,\chi_c\Big]^{1/2}, \tag{23}$$

both of which are the HQS singlets.

The higher excited states of J^P with $P = +$ can be constructed by the d-wave excitation as the total angular momentum. In this case, we have three possibilities as $(\ell_\lambda,\ell_\rho) = (2,0)$, $(1,1)$ and $(0,2)$. In the $(2,0)$ and $(0,2)$ cases, the diquark spin should be 0, and the total baryon spin can be $J = 3/2,\ 5/2$ as,

$$\Lambda_c^*(J^+;\ell_\lambda{=}2) = \Big[[\psi_{0d}(\vec{\lambda})\psi_{0s}(\vec{\rho}),d^0]^2,\chi_c\Big]^{J=2\pm1/2} D^0 c\ , \tag{24}$$

$$\Lambda_c^*(J^+;\ell_\rho{=}2) = \Big[[\psi_{0s}(\vec{\lambda})\psi_{0d}(\vec{\rho}),d^0]^2,\chi_c\Big]^{J=2\pm1/2} D^0 c\ , \tag{25}$$

In the case with $(\ell_\lambda,\ell_\rho) = (1,1)$, the diquark spin should be 1 as

$$\Lambda_c^*(J^+;\ell_\lambda=1,\ell_\rho=1) = \Big[[\psi_{0p}(\vec{\lambda})\psi_{0p}(\vec{\rho}),d^1]^j,\chi_c\Big]^{J} D^0 c\ . \tag{26}$$

The total angular momentum ℓ ($\vec{\ell} = \vec{\ell}_\lambda + \vec{\ell}_\rho$) can be 0, 1 and 2, and the resulting brown muck spin can be $j = (1)$, $(0,1,2)$, and $(1,2,3)$ giving 13 states. The heavy baryons are the HQS singlet only for $j = 0$ and the HQS doublet for the others.

We leave a comment on the difference between the wave function used in Ref. [31] and ours. In Ref. [31], the bases of the quark wave function are given by ${}^{2s+1}\ell_J$, namely

$$\Big[\big[\ell_\lambda\ell_\rho\big]^\ell[[s_1s_2]s_3\big]^s\Big]^J, \tag{27}$$

while ours are given by

$$\Big[\big[[\ell_\lambda\ell_\rho]^\ell[s_1s_2]^{s_{12}}\big]^j s_3\Big]^J. \tag{28}$$

They are different in general except for the highest weight state of ℓ and s. In the latter, the subcomponent $\big[[\ell_\lambda\ell_\rho]^\ell[s_1s_2]^{s_{12}}\big]^j$, which is assigned as the brown muck spin j, decouples from the heavy quark spin s_3 in the heavy quark limit. Hence the latter basis is compatible with the heavy quark symmetry.

III. FORMULATION

A. Basic interaction of the pion

In the constituent quark model, the pion can couple to a single quark through the Yukawa interaction, which is considered to contribute dominantly to one-pion emission decays (Fig. 3). In the relativistic description, there are two independent couplings of pseudo-scalar and axial-vector types,

$$\bar{q}\gamma_5\vec{\tau}q\cdot\vec{\pi},\quad \bar{q}\gamma_\mu\gamma_5\vec{\tau}q\cdot\partial^\mu\vec{\pi}\ . \tag{29}$$

In the non-relativistic model, they correspond to the following two terms,

$$\vec{\sigma}\cdot(\vec{p}_i+\vec{p}_f) = \vec{\sigma}\cdot\vec{q},\quad \vec{\sigma}\cdot(\vec{p}_i-\vec{p}_f)\ , \tag{30}$$

where $\vec{p}_i$ ($\vec{p}_f$) is the momentum of the initial (final) quarks and $\vec{q}$ is the pion momentum. We keep in mind that these two couplings in Eq. (29) are equivalent for the on-shell particles in the initial and final states, but not for the off-shell particles confined within a finite size. The present case is the latter, because the quarks are confined in the harmonic oscillator potential. In this work, we employ the axial-vector type coupling,

$$\mathcal{L}_{\pi qq}(x) = \frac{g_A^q}{2f_\pi}\bar{q}(x)\gamma_\mu\gamma_5\vec{\tau}q(x)\cdot\partial^\mu\vec{\pi}(x), \tag{31}$$

in accordance with the low-energy chiral dynamics. The non-relativistic limit in Eq. (31) leads to the combination of the two terms in Eq. (29). In Eq. (31), g_A^q is the axial coupling of the light quarks, for which we use the value $g_A^q = 1$ [39, 40]. As we will see later, importantly, the axial-vector coupling can explain surprisingly well the decay of $\Lambda_c^*(2595)$ through the time-derivative piece in Eq. (31). Contrary, the pseudoscalar coupling cannot reproduce it because it is proportional to the pion momentum q which almost vanishes. This strongly supports the chiral dynamics of the pion working with constituent light quarks.

B. Matrix elements with the quark model wave functions

In this section, we formulate the one-pion emission decay of a charmed baryon within the quark model. The relevant diagram is shown in Fig. 3, where one pion is emitted from a single light quark. We write state vector for the Y_c baryon ($Y_c = \Lambda_c$ or Σ_c) with mass M_{Y_c}, spin J and momentum P in the baryon rest frame in the momentum representation as,

$$|Y_c(P,J)\rangle = \sqrt{2M_{Y_c}}\sum_{\{s,\ell\}}\int\frac{d^3p_\rho}{(2\pi)^3}\int\frac{d^3p_\lambda}{(2\pi)^3} \frac{1}{\sqrt{2m}}\frac{1}{\sqrt{2m}}\frac{1}{\sqrt{2M}}\psi_{\ell_\rho}(\vec{p}_\rho)\psi_{\ell_\lambda}(\vec{p}_\lambda) |q_1(p_1,s_1)\rangle|q_2(p_2,s_2)\rangle|q_3(p_3,s_3)\rangle. \tag{32}$$

which is a superposition of quarks in the momentum space $|q_1(p_1,s_1)\rangle$, $|q_2(p_2,s_2)\rangle$, and $|q_3(p_3,s_3)\rangle$, weighted by the baryon wave functions $\psi_\rho(\vec{p}_\rho)$ and $\psi_\lambda(\vec{p}_\lambda)$. Here the relative momenta $\vec{p}_\rho$ and $\vec{p}_\lambda$ are defined by

$$\vec{p}_\lambda = \frac{1}{2m+M}(M\vec{p}_1 + M\vec{p}_2 - 2m\vec{p}_3) \tag{33}$$

$$\vec{p}_\rho = \frac{1}{2}(\vec{p}_1 - \vec{p}_2)\ . \tag{34}$$

and the total momentum of three quarks, which is the baryon momentum, is given by

$$\vec{P} = \vec{p}_1 + \vec{p}_2 + \vec{p}_3\ . \tag{35}$$

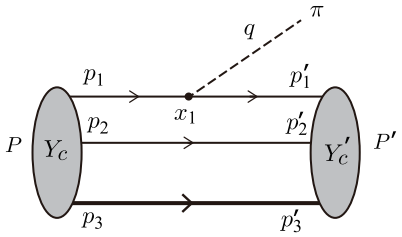

FIG. 3. Decay amplitude of the charmed baryon Y_c to Y_c' with one-pion emission.

The factors of $1/\sqrt{2m}$ are for the normalizations of the confined quark states so that $\int \frac{d^3p_j}{(2\pi)^3}|\psi(\vec{p}_j)|^2 = 1$. The sum $\sum_{\{s,\ell\}}$ is taken over the spins of the three quarks and their angular momenta such that the total angular momentum gives the spin J.

The decay amplitude for $Y_c \to Y_c'\pi$ is given by

$$\int d^4x_1 \langle Y_c'(P',J')\pi(q)|i\mathcal{L}(x_1)|Y_c(P,J)\rangle, \tag{36}$$

where only one light quark $|q_1\rangle$ in the initial and final baryon state participates in the transition as

$$\langle q_1'(p_1',s_1')\pi(q)|i\mathcal{L}_{\pi qq}(x_1)|q_1(p_1,s_1)\rangle \simeq i\frac{g_A^q}{2\pi}e^{i(p_1'-p_1+q)\cdot x_1}\times \left\{i\omega_\pi\langle\chi_{s_1'}|(\vec{p}_1+\vec{p}_1')\cdot\vec{\sigma}|\chi_{s_1}\rangle - i2m\langle\chi_{s_1'}|(\vec{p}_1-\vec{p}_1')\cdot\vec{\sigma}|\chi_{s_1}\rangle\right\}, \tag{37}$$

while the other light quark $|q_2\rangle$ and the charm quark $|q_3\rangle$ are spectators and then their matrix elements are just delta-functions of their three-momenta

$$\langle q_j'(p_j',s_j')|q_j(p_j,s_j)\rangle = 2E_j(2\pi)^3\delta^{(3)}(\vec{p}_j'-\vec{p}_j)\delta_{s_js_j'} = 2E_j\int d^3x_j e^{-i(\vec{p}_j'-\vec{p}_j)\cdot\vec{x}_j}\langle\chi_{s_j'}|\chi_{s_j}\rangle\ , \tag{38}$$

where $j=2$ or 3. We have now ten x-integrals as

$$\int dx_1^0 d^3x_1 d^3x_2 d^3x_3\ e^{i(p_1'-p_1+q)\cdot x_1}e^{-i(\vec{p}_2'-\vec{p}_2)\cdot\vec{x}_2}e^{-i(\vec{p}_3'-\vec{p}_3)\cdot\vec{x}_3}\ , \tag{39}$$

and the first x_1^0-integral leads to the energy conservation $(2\pi)\delta(E_1-E_1'-\omega_\pi)$ in $q_1 \to q_1'\pi$ process. We rewrite the remaining $\vec{x}$-integrals in terms of the Jacobi coordinates and we find

$$\int d^3X d^3\rho\, d^3\lambda e^{-i(\vec{P}'-\vec{P})\cdot\vec{X}}e^{-i(\vec{p}_\rho'-\vec{p}_\rho)\cdot\vec{\rho}}e^{-i(\vec{p}_\lambda'-\vec{p}_\lambda)\cdot\vec{\lambda}} \times e^{-i\vec{q}\cdot(\vec{X}+\frac{M}{2m+M}\vec{\lambda}+\frac{1}{2}\vec{\rho})}. \tag{40}$$

The $\vec{X}$-integral leads to the total three-momentum conservation, via $(2\pi)^3\delta^{(3)}(\vec{P}-\vec{P}'-\vec{q})$. By eliminating the common delta-functions for the energy-momentum conservation, we find the amplitude for $Y_c \to Y_c'\pi$ decay as

$$-it_{Y_c\to Y_c'\pi} = \sum_{\{\Lambda,\Sigma\}} i\frac{g_A^q}{2f_\pi}\sqrt{2M_{Y_c}}\sqrt{2M_{Y_c'}}\frac{1}{2m}\int\frac{d^3p_\rho}{(2\pi)^3}\int\frac{d^3p_\rho'}{(2\pi)^3}\int\frac{d^3p_\lambda}{(2\pi)^3}\int\frac{d^3p_\lambda'}{(2\pi)^3}\int d^3\lambda\int d^3\rho$$
$$\psi^*_{\ell_\rho'}(\vec{p}_\rho')e^{-i\vec{p}_\rho'\cdot\vec{\rho}}\psi_{\ell_\rho}(\vec{p}_\rho)e^{i\vec{p}_\rho\cdot\vec{\rho}}\psi^*_{\ell_\lambda'}(\vec{p}_\lambda')e^{-i\vec{p}_\lambda'\cdot\vec{\lambda}}\psi_{\ell_\lambda}(\vec{p}_\lambda)e^{i\vec{p}_\lambda\cdot\vec{\lambda}}e^{-i\vec{q}_\lambda\cdot\vec{\lambda}}e^{-i\vec{q}_\rho\cdot\vec{\rho}}$$
$$\left\{i\omega_\pi\langle\chi_{s_1'}|(\vec{p}_\lambda'+2\vec{p}_\rho')\cdot\vec{\sigma}|\chi_{s_1}\rangle + i\left(\omega_\pi\frac{M}{2m+M}-2m\right)\langle\chi_{s_1'}|\vec{\sigma}\cdot\vec{q}|\chi_{s_1}\rangle\right\}\langle\chi_{s_2'}|\chi_{s_2}\rangle\langle\chi_{s_c'}|\chi_{s_c}\rangle\ , \tag{41}$$

where the effective momentum transfer $\vec{q}_\lambda$ and $\vec{q}_\rho$ appearing in the pion plain wave $e^{-i\vec{q}\cdot\vec{x}_1}$ are defined by

$$\vec{q}_\lambda = \frac{M}{2m+M}\vec{q},\quad \vec{q}_\rho = \frac{1}{2}\vec{q}\ . \tag{42}$$

The first term in Eq. (41) involves the relative momenta $\vec{p}_\rho'$ and $\vec{p}_\lambda'$ of the constituent quarks in the final baryon, which can be replaced by the derivative of the wave functions as

$$\int\frac{d^3p_\rho'}{(2\pi)^3}\vec{p}_\rho'\psi^*_{\ell_\rho'}(\vec{p}_\rho')e^{-i\vec{p}_\rho'\cdot\vec{\rho}} = i\vec{\nabla}_\rho\int\frac{d^3p_\rho'}{(2\pi)^3}\psi^*_{\ell_\rho'}(\vec{p}_\rho')e^{-i\vec{p}_\rho'\cdot\vec{\rho}} = i\vec{\nabla}_\rho\psi^*_{\ell_\rho'}(\vec{\rho}), \tag{43}$$

and the same for $\vec{p}'_\lambda$. In the case of $\Lambda_c(JM)^+ \to \Sigma_c(J'M')^{++}\pi^-$, after performing the momentum integrals and by showing the flavor (isospin) part explicitly, the decay amplitude is given by

$$-it_{\Lambda_c^+\to\Sigma_c^{++}\pi^-} = -\frac{g_A^q}{2f_\pi}\sqrt{2M_{\Lambda_c}}\sqrt{2M_{\Sigma_c}}\frac{1}{2m}\int d^3\lambda\, d^3\rho\, e^{-i\vec{q}_\lambda\cdot\vec{\lambda}}e^{-i\vec{q}_\rho\cdot\vec{\rho}}\left\langle D^1 c\right|\tau^+_{(1)}\left|D^0 c\right\rangle$$
$$\left\langle [[\psi_{\ell_\lambda}(\lambda)\psi_{\ell_\rho}(\rho),d]^{j'},\chi_c]^{J'}_{M'}\right|\left\{\omega_\pi(i\overleftarrow{\nabla}_\lambda + 2i\overleftarrow{\nabla}_\rho)\cdot\vec{\sigma}_{(1)} + \left(\omega_\pi\frac{M}{2m+M} - 2m\right)\vec{\sigma}_{(1)}\cdot\vec{q}\right\}\left|[[\psi_{\ell_\lambda}(\lambda)\psi_{\ell_\rho}(\rho),d]^{j},\chi_c]^{J}_{M}\right\rangle, \quad (44)$$

where $\vec{\sigma}_{(1)}$ and $\tau^+_{(1)}$ matrices operate the spin and isospin wave functions of the quark-1. For simplicity, the notation for the bra and ket states

$$\left|[[\psi_{\ell_\lambda}(\lambda)\psi_{\ell_\rho}(\rho),d]^{j},\chi_c]^{J}_{M}\right\rangle \equiv \sum_{\{\ell,s\}}\psi_{\ell_\lambda}(\lambda)\psi_{\ell_\rho}(\rho)\left|\chi_{s_1}\right\rangle\left|\chi_{s_2}\right\rangle\left|\chi_{s_c}\right\rangle, \quad (45)$$

are used in Eq. (44). The derivatives $\overleftarrow{\nabla}_\lambda$ and $\overleftarrow{\nabla}_\rho$ operate the final state wave functions. We also have to consider the case that the pion couples to the another light quark $q_2(x_2)$. Summing over the amplitudes of the two cases coherently, we obtain the total decay amplitude.

C. Decay widths with the helicity amplitude

The decay width of $B_i \to B_f\pi$ is given by

$$\Gamma = \frac{1}{16\pi^2}\frac{q}{2M_i^2}\int d\Omega\sum_f\left|t_{B_i\to B_f\pi}\right|^2, \quad (46)$$

where q is the magnitude of the three-momentum of the final pion in the center-of-mass frame, and the sum is taken over the possible quantum numbers, in the present case, the spin state (helicity) of the final baryon for a given initial baryon spin. The matrix element depends on the decay angle Ω (the angle between the quantization axis of the initial baryon spin and the momentum vector $\vec{p}_f$ of the final baryon) and on the helicity of B_f. In this article, we employ the helicity amplitude approach to calculate the decay width in Eq. (46).

In this approach, we expand the initial spin state $|B_i(J,J_{z'}=J)\rangle_{z'}$, which is quantized along a fixed $\hat{e}_{z'}$ axis, in the angular momentum basis quantized along the direction of the momentum of the final baryon, $\hat{e}_z = \vec{p}_f/|\vec{p}_f|$, by

$$|B_i(J,J)\rangle_{z'} = \sum_M |B_i(J,M)\rangle_z D^J_{MJ}(-\phi,\theta,\phi)\ , \quad (47)$$

where D^J_{MJ} are the Wigner's D functions [41]. If the spin of the final state $\langle B_f(\vec{p}_f,h)|$ is quantized along $\hat{e}_z$, then the helicity h is equal to the third component of the final state spin,

$$\langle B_f(\vec{p}_f,h)| = {}_z\langle B_f(\vec{p}_f,J',h)|, \quad (48)$$

where J' is the spin of the final baryon B_f.

Hence the matrix element is written with its angular dependence as shown explicitly

$${}_{z'}\langle B_f(\vec{p}_f,J',h)\pi(-\vec{p}_f)|\,\hat{t}\,|B_i(J,J)\rangle_{z'} = D^J_{MJ}(-\phi,\theta,\phi)\,{}_z\langle B_f(\vec{p}_f,J',h)\pi(-\vec{p}_f)|\,\hat{t}\,|B_i(J,h)\rangle_z, \quad (49)$$

where only the diagonal element $M = h$ remains after summing over $\sum_M$, because of the helicity (spin z-component) conservation. In Eq. (49) both of the initial and final spins are quantized along $\hat{e}_z$ axis.

Now, the helicity amplitude A_h is defined by

$$(2\pi)^4\delta^{(4)}(P_f - P_i)A_h = {}_z\langle B_f(\vec{p}_f,J',h)\pi(-\vec{p}_f)|\,\hat{t}\,|B_i(J,h)\rangle_z\ . \quad (50)$$

The amplitude A_h depends on J, J' and h, but does not depend on the decay angle, because the spin quantization axis is chosen along the direction of the momentum of the final baryon $\vec{p}_f$, which is equal to the situation of the decay into the z-direction. The possible angular dependence of $\vec{p}_f$ is taken care of by the D function, and the angular-integral $d\Omega$ in Eq. (46) then can be performed exactly and finally we find

$$\Gamma = \frac{1}{4\pi}\frac{q}{2M_i^2}\frac{1}{2J+1}\sum_h|A_h|^2, \quad (51)$$

where $q = |\vec{p}_f|$. Here, the amplitude A_{-h} with the opposite helicity has the same form as A_h.

D. Parameters

In the present Hamiltonian of the harmonic oscillator in Eq. (1), we have three model-parameters; m the mass of the light quark, M that of the heavy quark, and k the spring constant. The masses of the quarks are set to be as,

$$m = 0.35 \pm 0.05\ (\text{GeV}), M = 1.5 \pm 0.1\ (\text{GeV}). \quad (52)$$

We tune the value of k so that the level spacing of the λ-mode excitation as $\omega_\lambda \sim 0.35 \pm 0.05$ GeV and the root-mean-square radius of the charmed baryon as $\sqrt{\langle R^2 \rangle} \sim$ 0.45–0.55 fm which is defined as the average of the distance of each quark from the center-of-mass as,

$$R^2 \equiv \frac{1}{3}\sum_{i=1}^{3}\left(\vec{r}_i - \vec{X}\right)^2 = \frac{1}{3}\left(\frac{2(2m^2+M^2)}{(2m+M)^2}\lambda^2 + \frac{1}{2}\rho^2\right), \quad (53)$$

We summarize the model parameters used in the present calculation in Table II. Depending on these input parameters, the range parameters of the Gaussian wave functions vary within the range of

$$a_\lambda = 0.36\text{–}0.44 \text{ (GeV)}, \quad a_\rho = 0.26\text{–}0.32 \text{ (GeV)}, \quad (54)$$

which is the source of the uncertainty in our theory predictions.

TABLE II. Range of the model parameters of $\{m, M, k\}$ (inputs) and the properties of resulting harmonic oscillator functions (outputs).

inputs	light quark mass m	0.3–0.4 (GeV)
	heavy quark mass M	1.4–1.6 (GeV)
	H.O. potential k	0.02–0.038 (GeV^3)
outputs	H.O. energy ω_λ	0.3–0.4 (GeV)
	H.O. energy ω_ρ	0.42–0.58 (GeV)
	gauss range a_λ	0.36–0.44 (GeV)
	gauss range a_ρ	0.26–0.32 (GeV)
	$\sqrt{\langle\lambda^2\rangle}$	0.55–0.67 (fm)
	$\sqrt{\langle\rho^2\rangle}$	0.76–0.93 (fm)
	$\sqrt{\langle R^2\rangle}$	0.45–0.55 (fm)

IV. NUMERICAL RESULTS

A. Decays of the ground state $\Sigma_c(1/2^+)$ and $\Sigma_c^*(3/2^+) \to \Lambda_c(1/2^+)\pi$

The $\Sigma_c(2455)$ baryon is an orbital ground state baryon having $J^P = 1/2^+$. The mass of the $\Sigma_c(2455)^{++}$ is 2453.97 ± 0.14 MeV and its full width is $1.89^{+0.09}_{-0.18}$ (MeV) [24]. The $\Sigma_c(2455) \to \Lambda_c(2286)\pi$ decay channel is the only possible strong decay and its branching ratio is $\sim$ 100%. The $\Sigma_c^*(2520)$ baryon has $J^P = 3/2^+$ and is expected to form a HQS doublet with $\Sigma_c(2455)$. The mass of the $\Sigma_c^*(2520)^{++}$ is $2518.41^{+0.21}_{-0.19}$ (MeV) and its width is $14.78^{+0.30}_{-0.40}$ (MeV) [24]. Again the $\Lambda_c(2286)\pi$ decay channel is the only possible channel in the strong decay and its branching ratio is $\sim$ 100%. Because both $\Sigma_c(2455)$ and $\Sigma_c^*(2520)$ baryons are the spin and isospin flip states of the ground state $\Lambda_c(2286)$, their decay rates reflect mainly the spin-isospin structure and is rather insensitive to the spatial structure. Therefore, we can use these processes to check the validity of the present quark model calculations.

The helicity amplitude for the $\Sigma_c(1/2^+) \to \Lambda_c(1/2^+)\pi$ decay is given by,

$$A_h = A_h^{\nabla\cdot\sigma} + A_h^{q\cdot,\sigma}, \quad (55)$$

where $A_h^{\nabla\cdot\sigma}$ and $A_h^{q\cdot\sigma}$ correspond to the $(\vec{\nabla}_\lambda + 2\vec{\nabla}_\rho)\cdot\vec{\sigma}$ term and the $\vec{q}\cdot\vec{\sigma}$ term in Eq. (44), respectively. They are given by

$$-iA_{1/2}^{\nabla\cdot\sigma} = G\frac{\omega_\pi}{m}\left(-\frac{1}{\sqrt{3}}\right)\left(\frac{1}{2}q_\lambda + q_\rho\right)F(q), \quad (56)$$

and

$$-iA_{1/2}^{q\cdot\sigma} = -G\frac{q}{m}\left(-\frac{1}{\sqrt{3}}\right)\left(\frac{M}{2m+M}\omega_\pi - 2m\right)F(q), \quad (57)$$

where $q_{\lambda(\rho)} \equiv |\vec{q}_{\lambda(\rho)}|$ and G denotes the coupling constant and the normalizations as,

$$G = \frac{g_A^q}{2f_\pi}\sqrt{2M_{\Lambda_c}}\sqrt{2M_{\Sigma_c}}\ . \quad (58)$$

The function $F(q)$ denotes the Gaussian form factor as

$$F(q) = e^{-q_\lambda^2/4a_\lambda^2}e^{-q_\rho^2/4a_\rho^2}\ , \quad (59)$$

which is the Fourier transform of ground to ground transition amplitude. The factors of a_λ and a_ρ correspond to the inverse of the range of the Gaussian wave functions for λ- and ρ-motions, respectively, and their definitions are given in Appendix. Similarly, the helicity amplitude for the $\Sigma_c^*(3/2^+) \to \Lambda_c(1/2^+)\pi$ decay is given by the same expressions as Eqs. (56) and (57) but the factor $-1/\sqrt{3}$ is replaced by $\sqrt{2/3}$ in both equations.

In Table III, we show the numerical results for the $\Sigma_c(2455)(1/2^+)^{++} \to \Lambda_c^+\pi^+$ decay. The calculated decay width is almost twice as large as the experimental value. We also show the results of $\Sigma_c^*(2520)(3/2^+)$ decay in the same table. The calculated decay width of $\Sigma_c^*(3/2^+)$ is again twice as large as the experimental value.

As shown in the table, the uncertainty from the ambiguities of the quark model parameters (m, M, k) is small, which means the decay width of the ground state to the ground state does not depend on the detail of the wave functions, as anticipated. Therefore the discrepancy might come from the axial-coupling constant g_A^q for the πqq interaction.

In the present calculation, we employ $g_A^q = 1$ for the $q\pi\pi$ coupling, but it is also known that this value does not reproduce the axial-coupling constant of the nucleon $g_A^N = 1.25$ but leads to $g_A^N = 5/3$ instead. To reproduce the axial-coupling constant of the nucleon g_A^N, one

TABLE III. Calculated decay widths of $\Sigma_c(2455)^{++}$ and $\Sigma_c^*(2520)^{++}$ into the $\Lambda_c(2286)^+\pi^+$ pair. q is the momentum of the final particle in center-of-mass frame.

B_i J^P (MeV)	$\Gamma_{\rm exp}$ (MeV)	q (MeV/c)	$\Gamma_{\rm th}(\Sigma_c(J^+)^{++} \to \Lambda_c(2286)^+\pi^+)$ (MeV)
$\Sigma_c(2455)^{++}$ $1/2^+$ (2453.98)	1.89	89	4.27–4.33
$\Sigma_c^*(2520)^{++}$ $3/2^+$ (2517.9)	14.78	177	30.3–31.6

needs a suppression factor of about 3/4 for g_A^q, which reduces the decay width by a factor $(3/4)^2 \sim 0.56$, the result of which is consistent with the experimental data. This is expected because the pion emission decays essentially measure the axial couplings for relevant baryons (transitions). Our input here is the axial coupling of the constituent quarks which can take in principle any value when chiral symmetry is spontaneously broken. Here we have shown that it is 3/4 empirically from the phenomena of the ground state baryons not only for the nucleon but also for charmed baryons, which is not far from the discussion of Weinberg [39]. The suppression of g_A has been considered to be originated from the mixing of p-waves due to relativistic corrections or pion clouds [42]. This, however, may vary for different baryon excitations. Keeping this in mind, in the following calculations for decays of the excited states, we keep using the value $g_A^q = 1$.

B. $\Lambda_c^*(2595)(1/2^-) \to \Sigma_c(2455)(1/2^+)\pi$

The $\Lambda_c^*(2595)^+$ baryon is the first excited charmed baryons with $I = 0$ and is expected to have $J^P = 1/2^-$. The total decay width is $\Gamma_{\rm exp} = 2.6 \pm 0.6$ MeV, where the $\Lambda_c^+\pi\pi$ channel is the only strong decay. The $\Lambda_c^+\pi\pi$ seems to be dominated by $\Sigma_c(2455)\pi$ and its branching ratio $\Gamma(\Sigma_c\pi)/\Gamma(\text{total})$ is quoted as $BR(\Sigma_c^{++}\pi^-) = BR(\Sigma_c^0\pi^+) = 24 \pm 7$ % [24]. The direct three-body decay width is $18 \pm 10\%$ which we do not calculate in this article.

Employing the quark model, we have three possibilities to describe the excited Λ_c^* baryon having $J^P = 1/2^-$ as discussed in the previous section. One is the λ-mode excitation having $j^P = 1^-$, and the other two are the ρ-mode excitations having $j^P = 0^-$ and $j^P = 1^-$.

The helicity amplitude for the π^- emission decay of $\Lambda_c^*(1/2^-;\lambda)^+ \to \Sigma_c(1/2^+)^{++}\pi^-$ is found again as the sum

$$A_h(1/2^-;\lambda) = A_h^{\nabla\cdot\sigma}(1/2^-;\lambda) + A_h^{q\cdot\sigma}(1/2^-;\lambda), \quad (60)$$

where

$$-iA_{1/2}^{\nabla\cdot\sigma}(1/2^-;\lambda) = iG\frac{\omega_\pi}{m}\left\{c_0 a_\lambda + c_2\left(\frac{1}{2}q_\lambda + q_\rho\right)\frac{q_\lambda}{a_\lambda}\right\}F(q), \quad (61)$$

and

$$-iA_{1/2}^{q\cdot\sigma}(1/2^-;\lambda) = -iG\frac{q}{m}\left(\frac{M}{2m+M}\omega_\pi - 2m\right)c_2\frac{q_\lambda}{a_\lambda}F(q), \quad (62)$$

where

$$c_0 = -\frac{1}{\sqrt{2}}, \quad c_2 = \frac{1}{3\sqrt{2}}, \quad (63)$$

which are determined by the Clebsch-Gordan coefficients. We summarize the general expressions in Appendix. We can see that, the $A^{\nabla\cdot\sigma}$ starts from $\mathcal{O}(q^0)$ reflecting properly the nature of possible s-wave decay, while $A^{q\cdot\sigma}$ is of order $\mathcal{O}(q^2)$. We will see that the former gives a considerable contribution to the $\Lambda_c^*(2595)$ decay width.

As for the ρ-mode with $j = 1$, we find a similar form for the $\Lambda_c^*(1/2^-,\rho_{j=1})^+ \to \Sigma(1/2^+)^{++}\pi^-$ decay as

$$-iA_{1/2}^{\nabla\cdot\sigma}(1/2^-;\rho_{j=1}) = iG\frac{\omega_\pi}{m}\left\{c_0 a_\rho + c_2\left(\frac{1}{2}q_\lambda + q_\rho\right)\frac{q_\rho}{a_\rho}\right\}F(q), \quad (64)$$

and

$$-iA_{1/2}^{q\cdot\sigma}(1/2^-;\rho_{j=1}) = -iG\frac{q}{m}\left(\frac{M}{2m+M}\omega_\pi - 2m\right)c_2\frac{q_\rho}{a_\rho}F(q), \quad (65)$$

where

$$c_0 = 2, \quad c_2 = -\frac{1}{3}. \quad (66)$$

In contrast to the above two cases, the situation is quite different for the decay of $\Lambda_c^*(1/2^-,\rho_{j=0})$ having the

brown muck spin $j = 0$. The amplitudes are exactly zero as,

$$A^{\nabla\cdot\sigma}_{1/2}(1/2^-;\rho_{j=0}) = 0, \tag{67}$$
$$A^{q\cdot\sigma}_{1/2}(1/2^-;\rho_{j=0}) = 0, \tag{68}$$

for the decay into $\Sigma_c(1/2^+)$ baryon. This is due to the spin conservation of the brown muck; the spin-parity $j^P = 0^-$ state cannot decay into $j^P = 1^+$ with the pion 0^- for any combination of relative angular momentum. Generally, as we will see more examples, such requirements lead to selection rules due to the consistency between the decays of baryons and decays of brown muck, or the diquark in the quark model because the pion couples only to the light quarks. Such observations can be done best by using the baryon wave functions as inspired by the heavy quark symmetry.

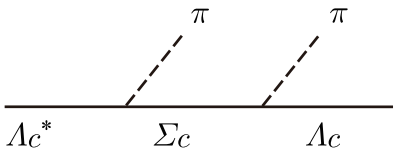

FIG. 4. Feynman diagram of the sequential decay of $\Lambda_c^* \to \Sigma_c\pi$ followed by $\Sigma_c \to \Lambda_c\pi$ supposed in Eq. (69).

To estimate the decay width of the $\Lambda_c^*(2595)$ baryon, we should take the finite width of the finial Σ_c baryon into account, because the $\Sigma_c\pi$ threshold is very close to the $\Lambda_c^*(2595)$ mass. Indeed, the $\Sigma_c^{++}\pi^-$ and $\Sigma_c^0\pi^+$ channels barely close at the $\Lambda_c^*(2595)$ mass while the $\Sigma_c^+\pi^0$ channel opens, which means the isospin breaking is large contrary to the assumption made in PDG [24]. To this end, we convolute the decay width of $\Lambda_c^*(2595)$ by the finite width of Σ_c as

$$\tilde{\Gamma}_{\Lambda_c^*} = \frac{1}{N}\int d\tilde{M}_{\Sigma_c}\,\mathrm{Im}\frac{\Gamma_{\Lambda_c^*}(\tilde{M}_{\Sigma_c})}{\tilde{M}_{\Sigma_c} - M_{\Sigma_c} + i\Gamma_{\Sigma_c}(\tilde{M}_{\Sigma_c})/2}, \tag{69}$$

where $\Gamma_{\Lambda^*}(\tilde{M}_\Sigma)$ is the calculated decay width of Λ_c^* given in Eq. (51) which depends on the mass $\tilde{M}_\Sigma$ of the final Σ_c baryon. The normalization factor N is defined by,

$$N = \int d\tilde{M}_{\Sigma_c}\,\mathrm{Im}\frac{1}{\tilde{M}_{\Sigma_c} - M_{\Sigma_c} + i\Gamma_{\Sigma_c}(\tilde{M}_{\Sigma_c})/2}\,. \tag{70}$$

We take into account the phase space factor for the Σ_c decay width in the convolution integral as,

$$\Gamma_\Sigma(\tilde{M}_{\Sigma_c}) = \Gamma_{\Sigma_c}\frac{M_{\Sigma_c}}{\tilde{M}_{\Sigma_c}}\left(\frac{\lambda^{1/2}(\tilde{M}^2_{\Sigma_c}, M^2_{\Lambda_c}, m^2_\pi)}{\lambda^{1/2}(M^2_{\Sigma_c}, M^2_{\Lambda_c}, m^2_\pi)}\right)^3 \times\theta(\tilde{M}_{\Sigma_c} - M_{\Lambda_c} - m_\pi), \tag{71}$$

where M_{Λ_c} is the mass of the ground state $\Lambda_c(2286)$, and Γ_{Σ_c} is the decay width of Σ_c given by $\Gamma_{\Sigma_c} = 1.89$ (MeV) for Σ_c^{++}, $\Gamma_{\Sigma_c} = 1.83$ (MeV) for Σ_c^0. Because only the upper limit is determined for Σ_c^+, we calculate the ratio of $\Gamma(\Sigma_c^{++})/\Gamma(\Sigma_c^+)$ by employing our formalism discussed in Sec. IV A, and then estimate it as $\Gamma_{\Sigma_c} = 2.1$ (MeV) for Σ_c^+. The convolution corresponds to the consideration of the sequential decay of the $\Lambda_c^* \to \Sigma_c\pi$ followed by $\Sigma_c \to \Lambda_c\pi$ as depicted in Fig. 4. The double π^0 emission decay of $\Lambda_c^*(2595)^+ \to \Lambda_c(2286)\pi^0\pi^0$ can be approximated by the convoluted single π^0 decay of $\Lambda_c^*(2595)^+ \to \Sigma_c(2455)^+\pi^0$ (including a symmetry factor for the two identical particles), because of the dominant contribution of the on-shell Σ_c [27]. Similarly, the charged pion decay $\Lambda_c\pi^+\pi^-$ is approximated by the sum of the $\Sigma_c^{++}\pi^-$ and $\Sigma_c^0\pi^+$ decays.

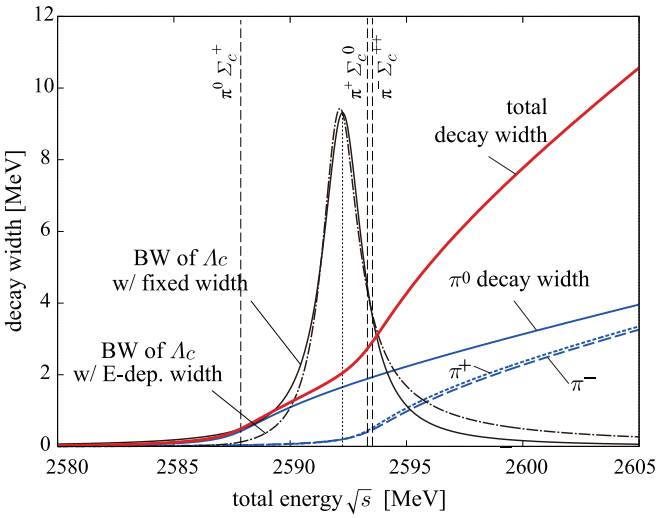

FIG. 5. (color online) Convoluted decay width of $\Lambda_c^*(2595;\lambda\text{-mode}) \to \Sigma_c(2455)\pi$ as functions of total energy (= the mass of the Λ_c^*). The thin (blue) lines denote the π^-, π^0, and π^+ emission decay widths as indicated in the figure. The thick (red) solid line denotes the sum of three charge states. The resulting Breit-Winger spectral functions of the Λ_c^* are also shown in arbitrary unit.

In Fig. 5, we show the calculated result for the decay width of the $\Lambda_c^*(2595)$ baryon in the case of the λ-mode as functions of the mass of the Λ_c^* (the total energy $\sqrt{s}$). We find that the $\pi^\pm$ decay width remains finite even at $\sqrt{s} = M_{\Lambda_c^*}$ which is below the $\pi^\pm$ threshold, owing to the finite width of the Σ_c baryon. We can also see that the π^0 threshold is located at 5 MeV below $\sqrt{s} = M_{\Lambda_c^*}$ and then the π^0 decay width is much larger than that of $\pi^\pm$, meaning a large isospin breaking. We also show the resulting Breit-Wigner form in Fig. 5 with the fixed width at $\sqrt{s} = M_{\Lambda_c^*} = 2592.25$ (MeV) and with the energy-dependent width. In the present case, both of the BW functions resemble because of the resulting small width. However, the energy-dependence of the width is large, so we have to be careful when estimating the BW width for $\Lambda_c^*(2595)$.

In Table IV we show the calculated decay widths of $\Lambda_c^*(2595)^+ \to \Sigma_c(2455)^{++}\pi^-$, $\Sigma_c(2455)^0\pi^+$, and

TABLE IV. Calculated decay width of the $\Lambda_c^*(2595) \to \Sigma_c(2455)\pi$. The charge decay channels are indicated in the table, where $[\Sigma_c\pi]^+$ denotes the isospin summed width. The quantum numbers of the λ- and ρ-modes are indicated by $(n_\lambda, \ell_\lambda)$ and (n_ρ, ℓ_ρ), and $J_{\Lambda_c^*}(j)^P$ stands for the assigned spin and parity for Λ_c^* with the brown muck spin j. The masses of the Λ_c^*, Σ_c, and π are also shown in the table. The symbol † indicates the closed channels for on-shell $\Sigma_c\pi$.

$\Lambda_c^*(2595)^+$ decay width ($M_{\Lambda^*} = 2592.25$ (MeV))

		decay channel	full	$[\Sigma_c\pi]^+$	$\Sigma_c^{++}\pi^-$	$\Sigma_c^0\pi^+$	$\Sigma_c^+\pi^0$
Experimental value $\Gamma_{\rm exp}$ (MeV) [24]			2.6 ± 0.6	-	0.624 (24%)	0.624 (24%)	-
momentum of final particle q (MeV/c)			-	-	†	†	29
this work	$(n_\lambda, \ell_\lambda)$, (n_ρ, ℓ_ρ)	$J_\Lambda(j)^P$					
Γ	$(0,1)$, $(0,0)$	$1/2(1)^-$		1.5–2.9	0.13–0.25	0.15–0.28	1.2–2.4
(MeV)	$(0,0)$, $(0,1)$	$1/2(0)^-$		0	0	0	0
		$1/2(1)^-$		6.5–11.9	0.57–1.04	0.63–1.15	5.3–9.7
			M_Σ (MeV)		2453.97	2453.75	2452.9
	input parameters employed		Γ_Σ (MeV)		1.89	1.83	2.1
	in the convolution Eq. (69)		m_π (MeV)		139.57	139.57	134.98

$\Sigma_c(2455)^+\pi^0$ together with the sum of these three channels evaluated at $\sqrt{s} = M_{\Lambda_c^*} = 2592.25$ (MeV). These numbers have uncertainty reflecting that of model parameters of (m, M, k) as discussed in Sec. III D. The uncertainty of the model parameters leads to almost factor-two difference in the decay widths. In spite of this uncertainty including the one coming from g_A^q, using the axial-vector coupling works well to reproduce the relatively large decay width of $\Lambda_c^*(2595)$ located at almost $\Sigma_c\pi$ threshold. This is due to the time derivative term with the strength determined the mass of the pion. Thus the decay of $\Lambda_c^*(2595)$ provides a good example to show that the chiral theory works up to the order $\mathcal{O}(m_\pi)$. As discussed in the previous section, we find that, by employing the pseudo-scalar coupling (γ_5) for the pion, we obtain less than 1 (keV) for the $\Lambda_c^*(2595)$ decay due to the small pion momentum q.

We also find that the assignment of the ρ-mode configuration with $j^P = 1^-$ to the $\Lambda_c^*(2595)$ leads to almost 2.5 – 5 times larger width than the experimental value for the total width. They are significantly large even if we consider the uncertainty of the pion coupling, because the experimental total width contains not only the $\Sigma_c\pi$ decay channel but also the non-resonant three-body decay of $\Lambda_c\pi\pi$ which we do not consider in this paper.

In addition, the ρ-mode configuration with $j^P = 0^-$ cannot decay into $\Sigma_c\pi$. Therefore we can conclude that, by the detailed study of decay width, it is likely that $\Lambda_c^*(2595)$ baryon is dominated by the λ-mode configuration as expected. We might add a comment that other assignments of the $J^P = 3/2^-$ or higher spin configurations for $\Lambda_c^*(2595)$ cannot reproduce the large experimental value for the decay width due to d-wave (or higher partial wave) nature.

C. $\Lambda_c^*(2625)(3/2^-) \to \Sigma_c(2455)(1/2^+)\pi$

TABLE V. Calculated decay widths of the $\Lambda_c^*(2625) \to \Sigma_c(2455)^{++}\pi^-$. The quantum numbers of the λ- and ρ-mode are indicated by $(n_\lambda, \ell_\lambda)$ and (n_ρ, ℓ_ρ), and $J_{\Lambda_c^*}(j)^P$ stands for the assigned spin and parity for Λ_c^* with the brown muck spin j. The masses of the Σ_c^{++} and π^- are $M_{\Sigma_c^{++}} = 2453.97$ (MeV) and $m_{\pi^-} = 139.57$ (MeV).

$\Lambda_c^*(2625)^+$ decay width ($M_{\Lambda^*} = 2628.11$ (MeV))

		decay channel	full	$\Sigma_c^{++}\pi^-$
Experimental value $\Gamma_{\rm exp}$ (MeV) [24]			< 0.97	$< 0.05 (< 5\%)$
momentum of final particle q (MeV/c)			-	101
this work	$(n_\lambda, \ell_\lambda)$, (n_ρ, ℓ_ρ)	$J_\Lambda(j)^P$		
Γ	$(0,1)$, $(0,0)$	$1/2(1)^-$		5.4–10.7
(MeV)		$3/2(1)^-$		0.024–0.039
	$(0,0)$, $(0,1)$	$1/2(0)^-$		0
		$1/2(1)^-$		24.0–45.1
		$3/2(1)^-$		0.013–0.019
		$3/2(2)^-$		0.023–0.034
		$5/2(2)^-$		0.010–0.015

The $\Lambda_c^*(2625)^+$ baryon is very narrow resonant state and is expected to have $J^P = 3/2^-$. In PDG, only the upper limit of the decay width is given as $\Gamma_{\rm exp} < 0.97$ MeV [24]. The $\Lambda_c^+\pi\pi$ and its submode $\Sigma_c\pi$ are the only strong decay channel. The branching ratio $BR(\Sigma_c^{++}\pi^-)/BR(\Lambda_c^+\pi^+\pi^-)$ is less than 5%, and therefore the partial decay width for $\Gamma_{\rm exp}(\Lambda_c^*(2625)^+ \to \Sigma_c^{++}\pi^-)$ is less than 0.05 MeV.

As discussed in the previous section, the $\Lambda_c^*(2625)$ baryon is assigned to be the low-lying orbital excitation

state with $\ell_\lambda = 1$ with spin-0 light diquark. The helicity amplitude for the $\Lambda_c^*(3/2^-;\lambda)^+ \to \Sigma_c^{++}\pi^-$ is then given by the same expressions as Eqs. (61) and (62) but with the different coefficients as

$$c_0 = 0, \quad c_2 = -\frac{1}{3} \ . \tag{72}$$

In contrast to the case of $\Lambda_c^*(2595)$, the coefficient c_0 of the q^0 term is zero then the helicity amplitudes $A_h^{\nabla\cdot\sigma}$ and $A_h^{q\cdot\sigma}$ are of order of $\mathcal{O}(q^2)$ as expected for the $3/2^- \to 1/2^+ + 0^-$ decay.

We have two more possible quark configurations for the Λ_c^* excitations with $J^P = 3/2^-$, which are the ρ-mode excitations with $j = 1$ and $j = 2$. The helicity amplitudes for these configurations are found to be again the same as Eqs. (64) and (65) but with different coefficients as

$$c_0 = 0, \quad c_2 = -\frac{1}{3\sqrt{2}}, \tag{73}$$

for $\Lambda_c^*(3/2^-, \rho_{j=1}) \to \Sigma_c(1/2^+)\pi$ decay, and

$$c_0 = 0, \quad c_2 = \frac{1}{\sqrt{10}}, \tag{74}$$

for $\Lambda_c^*(3/2^-, \rho_{j=2}) \to \Sigma_c(1/2^+)\pi$ decay.

In Table V we show the numerical results for the $\Lambda_c^*(2625)^+ \to \Sigma_c(2455)^{++}\pi^-$ decay. In the $\Lambda_c^*(2625)$ case, we do not convolute over the finite width of Σ_c because the $\Sigma_c\pi$ threshold is well below the $\Lambda_c^*(2625)$ mass, and the convolution does not change the result much. In the table, we also show the calculated decay widths of other assignments than $J^P = 3/2^-$.

We find that the assignment of λ-mode configuration with $J^P = 3/2^-$ for $\Lambda_c^*(2625)$ works very well to describe the small decay width of the $\Lambda_c^*(2625) \to \Sigma_c\pi$, while the assignment of $1/2^-$ leads to larger width than the experimental value. In contrast to the case of $\Lambda_c^*(2595)(1/2^-)$, however, we cannot exclude the possibilities of the ρ-mode configurations for $\Lambda_c^*(2625)(3/2^-)$ by the study of decay width, because the calculated $\Sigma_c\pi$ decay widths for λ-mode and two ρ-modes with $J = 3/2^-$ are accidentally similar to each other. It is interesting, however, that these three modes give quite different transition amplitudes for the $\Sigma_c^*(3/2^+)\pi$ decay as will be discussed later in Sec. IV D, although the $\Sigma_c^*\pi$ channel is closed for $\Lambda_c^*(2625)$. To discuss the structure of $\Lambda_c^*(2625)$ in more detail, we need systematical analyses of the mass spectrum [23], non-resonant three-body decay, and so on.

D. Decays of the higher excited Λ_c^* baryons

In Ref. [24], three more Λ_c^* states are nominated, $\Lambda_c^*(2765)$, $\Lambda_c^*(2880)$, and $\Lambda_c^*(2940)$, though $\Sigma_c^*(2765)$ cannot be excluded for $\Lambda_c^*(2765)$. Among them, spin of $\Lambda_c^*(2880)$ is the only quantum number that is well determined in experiment. The parity of $\Lambda_c^*(2880)$ is assigned to be positive, but it deserves being carefully examined. Therefore we consider possible assignments of both positive and negative parity cases. For these higher states, the $\Sigma_c^*(2520)\pi$ channel opens in addition to the $\Sigma_c(2450)\pi$ channel. The ratio of $\Gamma(\Sigma_c^*\pi)/\Gamma(\Sigma_c\pi)$ also can help us to determine the quantum numbers, and the quark configuration as well. In the following discussions, $\Sigma_c^{(*)}$ denotes $\Sigma_c(2455)$ with $1/2^+$ or $\Sigma_c^*(2520)$ with $3/2^+$.

1. $\Lambda_c^*(2765) \to \Sigma_c^{(*)}\pi$ decay

The $\Lambda_c^*(2765)$ baryon is seen in $\Lambda_c^+\pi^+\pi^-$ channel as a broad peak [24, 43]. The width is reported as $\Gamma_{\rm exp} = 50$ (MeV), but its quantum numbers are still unknown. For this baryon, we consider the p-wave excitations in λ- or ρ-mode with negative parity; $\{(n_\lambda, \ell_\lambda), (n_\rho, \ell_\rho)\} = \{(0,1),(0,0)\}$ or $\{(0,0),(0,1)\}$. We also consider the possibility of s-wave or d-wave excitations in λ-mode with positive parity; $\{(n_\lambda, \ell_\lambda), (n_\rho, \ell_\rho)\} = \{(1,0),(0,0)\}$ or $\{(0,2),(0,0)\}$. Further studies on $\Lambda_c^*(2765)$ with other quark configurations are in progress and will be discussed elsewhere [44].

In Table VI, we summarize the possible Λ_c^* spin-parity considered here together with the calculated results. Because the partial decay widths are not measured yet, we show the isospin summed width calculated by using the isospin-averaged masses $M_{\Sigma_c^{(*)}}$ and m_π. The concrete forms of the helicity amplitudes are summarized in Appendix. We find that, for higher j, the decay width tends to be smaller due to the suppression of the phase space for higher relative angular momentum in the final state.

In the last column in Table VI, we also show the ratio of the decay widths to $\Sigma_c(2455)\pi$ and $\Sigma_c^*(2520)\pi$ defined by

$$R = \frac{\Gamma(\Lambda_c^* \to \Sigma_c^*\pi)}{\Gamma(\Lambda_c^* \to \Sigma_c\pi)} \ . \tag{75}$$

We find the order of magnitudes of the ratio R are quite different for different configurations even if the spin-parity is the same, e.g. $J_{\Lambda_c^*}(j)^P = 3/2(1)^-(\lambda\text{-mode})$, $3/2(1)^-(\rho\text{-mode})$ and $3/2(2)^-(\rho\text{-mode})$. In fact, these three modes give the similar widths for the $\Sigma_c\pi$ decay as discussed in the previous section, but give quite different widths for $\Sigma_c^*\pi$. In principle, the $\Lambda_c^*(3/2^-)$ baryon can decay by s-wave to $\Sigma_c^*(3/2^+)\pi(0^-)$, while it decays by d-wave to $\Sigma_c(1/2^+)\pi(0^-)$. Then the ratio R can be expressed by

$$R = \frac{\Gamma(\Sigma_c^*\pi)_s + \Gamma(\Sigma_c^*\pi)_d}{\Gamma(\Sigma_c\pi)_d}, \tag{76}$$

which is, in general, larger than unity. This is the case for the $J_{\Lambda_c^*}(j)^P = 3/2(1)^-$ as

$$R(3/2(1)^-(\lambda\text{-mode})) = 5.6\text{–}7.8 \ , \tag{77}$$

$$R(3/2(1)^-(\rho\text{-mode})) = 49\text{–}70 \ . \tag{78}$$

In contrast, the brown muck $j^P = 2^-$ state cannot decay by s-wave to the brown muck 1^+ state in $\Sigma_c^*(3/2^+)\pi(0^-)$

TABLE VI. Calculated decay widths of the $\Lambda_c^*(2765) \to \Sigma_c(2455)\pi$ and $\to \Sigma_c^*(2520)\pi$. The quantum numbers of the λ- and ρ-modes are indicated by $(n_\lambda, \ell_\lambda)$ and (n_ρ, ℓ_ρ), and $J_{\Lambda_c^*}(j)^P$ stands for the assigned spin and parity for Λ_c^* with the brown muck spin j. $[\Sigma_c^{(*)}\pi]^+$ denotes the isospin summed width calculated by using the isospin average masses $M_{\Sigma_c} = 2453.5$ (MeV), $M_{\Sigma_c^*} = 2518.1$ (MeV), and $m_\pi = 138.0$ (MeV). The ratio R indicates the Σ_c^*/Σ_c defined in the text.

$\Lambda_c^*(2765)^+$ decay width ($M_{\Lambda^*} = 2766.6$ (MeV))

	decay channel	full	$[\Sigma_c^{(*)}\pi]_{\rm total}$	$[\Sigma_c\pi]^+$	$[\Sigma_c^*\pi]^+$	R
Experimental value $\Gamma_{\rm exp}$ (MeV)		50 [24]		-	-	-
momentum of final particle q (MeV/c)				265	197	
	(n_λ,ℓ_λ), (n_ρ,ℓ_ρ)	$J_\Lambda(j)^P$				
	$(0,1)$, $(0,0)$	$1/2(1)^-$	65.1–146.3	61.2–140.2	3.9–6.1	0.044–0.064
		$3/2(1)^-$	52.2–104.2	7.9–11.9	44.3–92.4	5.6–7.8
	$(0,0)$, $(0,1)$	$1/2(0)^-$	0	0	0	-
this work		$1/2(1)^-$	325.8–676.3	323.7–673.3	2.1–3.0	0.0044–0.0064
Γ		$3/2(1)^-$	210.4–413.5	4.2–5.8	206.2–407.7	49–70
(MeV)		$3/2(2)^-$	9.4–13.1	7.6–10.5	1.9–2.7	0.25–0.26
		$5/2(2)^-$	6.3–8.8	3.4–4.7	2.9–4.2	0.87–0.90
	$(1,0)$, $(0,0)$	$1/2(0)^+$	1.6–4.5	0.86–2.49	0.78–1.98	0.79–0.91
	$(0,2)$, $(0,0)$	$3/2(2)^+$	4.7–10.9	4.4–10.1	0.33–0.72	0.071–0.076
		$5/2(2)^+$	1.9–4.4	0.13–0.32	1.77–4.04	12.8–13.8

because of the spin-parity conservation. This is another example of the selection rules in the heavy quark limit. Due to the absence of s-wave contribution, the ratio R is smaller than unity for $3/2(2)^-$ as

$$R(3/2(2)^-(\rho\text{-mode})) = \frac{\Gamma(\Sigma_c^*\pi)_d}{\Gamma(\Sigma_c\pi)_d} = 0.25\text{–}0.26\ . \quad (79)$$

In this configuration, the amplitudes of $\Sigma_c\pi$ and $\Sigma_c^*\pi$ decays are the same except the momentum q of pion as discussed in Ref. [3]. Here, we stress that the s-wave suppression for $J^P_{\Lambda_c^*} = 3/2^-$ is found only in the case of $j^P = 2^-$, and not in the other quark configurations. This is the same phenomenon that the $1/2(0)^-$ state cannot decay into $\Sigma_c^{(*)}\pi$ as mentioned in Sec. IV B, and also is seen for the decay of the $\Lambda_c^*(2880)$ as discussed in the next section.

As for the magnitude of the decay width, we find that the assignments of $J_{\Lambda_c^*}(j)^P = 1/2(1)^-$ and $3/2(1)^-$ ($\ell_\rho = 1$) give rather large decay widths due to the s-wave nature into either $\Sigma_c(1/2^+)\pi$ or $\Sigma_c^*(3/2^+)\pi$. We can exclude these assignments because the resulting decay widths are too large. Calculated widths for λ-modes ($\ell_\lambda = 1$) are slightly larger as compared with the observed full width, which does not seem inconsistent if we consider the uncertainty of g_A^q . However, by taking into account contributions of decays into non-resonant three-body $\Lambda\pi\pi$, these λ-mode states will receive a larger full width, with which the possibility for them to be identified with $\Lambda_c^*(2765)$ might decrease.

Among the considered assignments in this article, the other assignments $J_{\Lambda_c^*}(j)^P = 1/2(0)^-$, $1/2(0)^+$, $3/2(2)^-$, $3/2(2)^+$, $5/2(2)^-$ and $5/2(2)^+$ cannot be excluded because the total $\Sigma_c^{(*)}\pi$ decay width is consistent with the experimental value. The ratio R, however, takes different value reflecting the structure of the Λ_c^* baryon which will help to determine the quantum numbers.

2. $\Lambda_c^*(2880) \to \Sigma_c^{(*)}\pi$ decay

The $\Lambda_c(2880)$ charmed baryon is observed in $\Lambda_c\pi\pi$ channel [38, 43] as well as in pD^0 channel [45]. The spin is determined as 5/2 from the angular distribution of the decay into $\Sigma_c(2455)\pi$ [38]. In PDG [24], the parity is assigned to be positive from the analysis of Σ_c^*/Σ_c branching ratio in comparison with the prediction of the chiral perturbation [30] with the heavy quark symmetry [3]. However, as discussed in [30] a subtlety arises when calculating the ratio.

In Table VII we summarize the quark configurations considered here for $\Lambda_c^*(2880)$. By comparing the observed full width $\Gamma_{\rm exp} = 5.8$ MeV and calculated total one-pion decay width, we can exclude all of the p-wave configurations with the negative parity including $5/2^-$. As for $5/2^-$ with ρ-mode excitation, both of the decays $\Lambda_c^*(5/2^-) \to \Sigma_c(1/2^+)\pi$ and $\Lambda_c^*(5/2^-) \to \Sigma_c^*(3/2^+)\pi$ ($(j^P = 2^-) \to (j^P = 1)^+0^-$ in terms of the brown muck) go through by d-wave, and the Σ_c^*/Σ_c ratio R is larger than unity as,

$$R(5/2(2)^-;\rho) = 1.6\text{–}1.8, \quad (80)$$

which does not agree with the experimental value $R = 0.225 \pm 0.062 \pm 0.010$ [38]. This conclusion is consistent

TABLE VII. Calculated decay width of the $\Lambda_c^*(2880) \to \Sigma_c(2455)\pi$ and $\to \Sigma_c^*(2520)\pi$. The quantum numbers of the λ- and ρ-modes are indicated by $(n_\lambda, \ell_\lambda)$,$(n_\rho, \ell_\rho)$, and $J_{\Lambda_c^*}(j)^P$ stands for the assigned spin for Λ_c^* with the brown muck spin j and the parity P. For the $\{(0,1),(0,1)\}$ configurations, we also show the total angular momentum $\vec{\ell} = \vec{\ell}_\lambda + \vec{\ell}_\rho$ as a subscript ℓ in $J_{\Lambda_c^*}(j)^P_\ell$. $[\Sigma_c^{(*)}\pi]^+$ denotes the isospin summed width calculated by using the isospin average masses $M_{\Sigma_c} = 2453.5$ (MeV), $M_{\Sigma_c^*} = 2518.1$ (MeV), and $m_\pi = 138.0$ (MeV). The ratio R indicates the Σ_c^*/Σ_c defined in the text.

$\Lambda_c^*(2880)^+$ decay width ($M_{\Lambda^*} = 2881.53$ (MeV))

		decay channel	full	$[\Sigma_c^{(*)}\pi]_{\rm total}$	$[\Sigma_c\pi]^+$	$[\Sigma_c^*\pi]^+$	R
	Experimental value $\Gamma_{\rm exp}$ (MeV)		5.8 ± 1.1 [24]				0.225 [38]
	momentum of final particle q (MeV/c)				375	315	
	$(n_\lambda, \ell_\lambda)$, (n_ρ, ℓ_ρ)	$J_\Lambda(j)^P$					
	$(0,1)$, $(0,0)$	$1/2(1)^-$		111.9–254.8	76.9–204.0	35.0–50.8	0.25–0.46
		$3/2(1)^-$		129.6–248.8	37.7–52.1	91.9–196.7	2.4–3.8
	$(0,0)$, $(0,1)$	$1/2(0)^-$		0	0	0	-
this work		$1/2(1)^-$		502.5–1129.7	483.9–1104.7	18.6–24.9	0.038–0.023
Γ		$3/2(1)^-$		439.3–919.5	20.0–25.6	419.3–893.9	21–35
(MeV)		$3/2(2)^-$		52.8–68.5	36.0–46.0	16.7–22.4	0.46–0.49
		$5/2(2)^-$		42.0–55.3	16.0–20.5	26.0–34.9	1.6–1.7
	$(1,0)$, $(0,0)$	$1/2(0)^+$		3.7–13.5	1.3–5.6	2.4–7.9	1.4–1.8
	$(0,2)$, $(0,0)$	$3/2(2)^+$		16.3–39.5	13.9–34.2	2.4–5.3	0.16–0.17
		$5/2(2)^+$		11.2–26.1	1.2–2.8	9.9–23.3	8.1–8.4
	$(0,0)$, $(1,0)$	$1/2(0)^+$		16.5–40.2	7.0–18.2	9.5–22.1	1.2–1.4
	$(0,0)$, $(0,2)$	$3/2(2)^+$		44.8–85.4	39.5–76.0	5.3–9.4	0.12–0.13
		$5/2(2)^+$		27.8–52.2	1.4–2.6	26.4–49.5	18.7–18.9
	$(n_\lambda, \ell_\lambda)$, (n_ρ, ℓ_ρ)	$J_\Lambda(j)^P_\ell$					
	$(0,1)$, $(0,1)$	$5/2(2)^+_2$		51.7–109.6	1.8–3.5	49.9–106.1	27.5–30.1
		$5/2(2)^+_1$		0.63–1.68	0	0.63–1.68	(∞)
		$5/2(3)^+_2$		2.9–5.8	2.1–4.0	0.85–1.73	0.41–0.43

with the chiral perturbation calculation with heavy quark symmetry [3, 30].

For the spin-parity $5/2^+$ case, we can consider five configurations as shown in Table VII; one d-wave excitation in λ-motion ($5/2(2)^+$ with $\ell_\lambda = 2$, denoted by $\lambda\lambda$), the one in ρ-motion ($5/2(2)^+$ with $\ell_\rho = 2$, denoted by $\rho\rho$), and three double-p-wave excitations in λ- and ρ-motions ($J_\Lambda(j)^P_\ell = 5/2(2)^+_1$, $5/2(2)^+_2$, $5/2(3)^+_2$ where $\vec{\ell} = \vec{\ell}_\ell + \vec{\ell}_\rho$ with $(\ell_\lambda, \ell_\rho) = (1,1)$, denoted by $\lambda\rho$). Some of these configurations give consistent decay width with the observed full width $\Gamma_{\rm exp} = 5.8$ (MeV). As for the Σ_c^*/Σ_c ratio, however, we obtain considerably different values for different configurations like,

$$\begin{aligned} R(5/2(2)^+;\lambda\lambda) &= 8.1\text{–}8.4\ , \\ R(5/2(2)^+;\rho\rho) &= 18.7\text{–}18.9\ , \\ R(5/2(2)^+_2;\lambda\rho) &= 27.5\text{–}30.1\ , \\ R(5/2(2)^+_1;\lambda\rho) &= (\infty)\ , \\ R(5/2(3)^+_2;\lambda\rho) &= 0.41\text{–}0.43\ , \end{aligned} \tag{81}$$

where the ambiguities of model parameters are almost canceled. Note that (∞) for $5/2(2)^+_1(\lambda\rho)$ state is due to the zero decay width into $\Sigma_c\pi$. Among these five configurations, we find that *only one* configuration $(5/2(3)^+_2;\lambda\rho)$ with the brown muck spin $j = 3$ with $\ell = 2$ agrees both with the small ratio $R < 1$ and with the magnitude of total decay width. This seems to contrast with the calculation in Ref. [30], where the other quark configuration for $5/2^+$ also gives the small R.

This discrepancy can be explained as follows. The decay of $\Lambda_c^*(5/2^+) \to \Sigma_c(1/2^+)\pi$ goes through only by the f-wave in the final two-body state, while the decay $\Lambda_c^*(5/2^+) \to \Sigma_c^*(3/2^+)\pi$ can go through both by f and p-waves. The discussion based on the heavy quark limit leading to the model independent relation is possible only when the same f-waves are taken, which is completely contaminated by the presence of the p-wave contribution. As shown explicitly in Appendix, the amplitude for $\Lambda_c^*(5/2^+) \to \Sigma_c^*(3/2^+)\pi$ can contain the p-wave contribution (c_1 term in Eq. (B6)). Thus we have

$$R(5/2^+) = \frac{\Gamma(\Sigma_c^*\pi)_p + \Gamma(\Sigma_c^*\pi)_d}{\Gamma(\Sigma_c\pi)_d} > 1, \tag{82}$$

except the case of $5/2(3)^+_2$. Only for the case of $5/2(3)^+_2$,

TABLE VIII. Calculated decay width of the $\Lambda_c^*(2940) \to \Sigma_c(2455)\pi$ and $\to \Sigma_c^*(2520)\pi$. The quantum numbers of the λ- and ρ-modes are indicated by $(n_\lambda, \ell_\lambda)$,$(n_\rho, \ell_\rho)$, and $J_{\Lambda_c^*}(j)^P$ stands for the assigned spin for Λ_c^* with the brown muck spin j and the parity P. For the $\{(0,1),(0,1)\}$ configurations, we also show the total angular momentum $\vec{\ell} = \vec{\ell}_\lambda + \vec{\ell}_\rho$ as a subscript ℓ in $J_{\Lambda_c^*}(j)^P_\ell$. $[\Sigma_c^{(*)}\pi]^+$ denotes the isospin summed width calculated by using the isospin average masses $M_{\Sigma_c} = 2453.5$ (MeV), $M_{\Sigma_c^*} = 2518.1$ (MeV), and $m_\pi = 138.0$ (MeV). The ratio R indicates the Σ_c^*/Σ_c defined in the text.

$\Lambda_c^*(2940)^+$ decay width ($M_{\Lambda^*} = 2939.3$ (MeV))

	decay channel	full	$[\Sigma_c^{(*)}\pi]_{\rm total}$	$[\Sigma_c\pi]^+$	$[\Sigma_c^*\pi]^+$	R
	Experimental value Γ (MeV)	17^{+8}_{-6} [24]		(seen)	-	
	momentum of final particle q (MeV/c)			427	369	
	(n_λ,ℓ_λ), (n_ρ,ℓ_ρ)	$J_\Lambda(j)^P$				
	$(0,1)$, $(0,0)$	$1/2(1)^-$	144.8–313.8	73.8–215.4	71.0–98.4	0.46–0.96
		$3/2(1)^-$	182.2–332.0	65.4–85.7	116.8–246.3	1.8–2.9
	$(0,0)$, $(0,1)$	$1/2(0)^-$				
this work		$1/2(1)^-$	557.0–1299.3	519.3–1250.9	37.6–48.3	0.039–0.072
Γ		$3/2(1)^-$	536.5–1152.9	34.6–42.2	501.8–1110.7	15–26
(MeV)		$3/2(2)^-$	96.2–119.4	62.3–75.9	33.9–43.5	0.54–0.57
		$5/2(2)^-$	80.4–101.4	27.7–33.7	52.7–67.7	1.9–2.0
	$(1,0)$, $(0,0)$	$1/2(0)^+$	3.7–17.4	1.1–6.4	2.7–11.0	1.7–2.5
	$(0,2)$, $(0,0)$	$3/2(2)^+$	24.9–61.7	20.1–51.0	4.8–10.8	0.21–0.24
		$5/2(2)^+$	19.8–46.6	2.8–5.9	17.1–40.7	6.2–6.9
	(n_λ,ℓ_λ), (n_ρ,ℓ_ρ)	$J_\Lambda(j)^P_\ell$				
	$(0,1)$, $(0,1)$	$7/2(3)^+_2$	5.8–11.1	2.6–4.8	3.2–6.2	1.22–1.29

p-wave contribution ($\tilde{c}_1$ term in Eq. (B7)) is zero because of the conservation of the brown muck spin-parity; the brown muck of 3^+ cannot decay into 1^+ with the pion 0^- in p-wave, which leads to

$$R(5/2(3)^+_2; \lambda\rho) = \frac{\Gamma(\Sigma_c^*\pi)_d}{\Gamma(\Sigma_c\pi)_d} < 1 \ . \tag{83}$$

We stress here again that the p-wave suppression is found only in the case of $5/2(3)^+$ with $\ell = 2$, and not in the other states with $5/2^+$. Here it is worth to mention that the $\mathcal{O}(q^1)$ contribution, which allows us to distinguish the possible quark configurations for the same spin-parity, appears only in $A^{\nabla\cdot\sigma}$ term arising from the axial-vector coupling $\gamma_\mu\gamma_5$ of the pion.

If $\Lambda_c^*(2880)$ is assigned as a $\lambda\rho$-mode state, a question arises where the $\lambda\lambda$-mode states with $\ell_\lambda = 2$ are. Excitation energies of the $\lambda\lambda$-mode states are expected to be lower than those of the $\lambda\rho$-mode states. Other information such as production rates as discussed in Ref. [46] is helpful to solve this problem, for which an experimental measurement is planned in J-PARC [47].

3. $\Lambda_c(2940) \to \Sigma_c^{(*)}\pi$ decay

As for $\Lambda_c^*(2940)$, a narrow peak is observed both in pD^0 channel [45] and in $\Sigma_c\pi$ channel [38]. The total width is $\Gamma_{\rm exp} = 17^{+8}_{-6}$ (MeV) [24]. The spin-parity is not determined.

In Table VIII, we show the calculated one-pion decay widths together with the considered quark configurations for $\Lambda_c^*(2940)$. In the previous section, we pointed out the possibility that $\Lambda_c^*(2880)$ is $5/2(3)^+_2$ excitation. If this is the case, a new question arises; which Y_c baryon is the partner of the HQS doublet possessing $7/2(3)^+_2$. To discuss the possibility of $\Lambda_c^*(2940)$ being the doublet partner of $\Lambda_c^*(2880)$, we also show the one-pion decay width with the $7/2(3)^+_2$ assignment for $\Lambda_c^*(2940)$ in the last line of Table VIII. We can see that this assignment can be consistent with the experimental full width in [24] in the sense that the calculated total one-pion emission decay width does not exceed the reported full width. For the same reason, the negative parity assignments can be excluded for the $\Lambda_c^*(2940)$. Similarly to other Λ_c^* baryons, the partial decay widths and/or the Σ_c^*/Σ_c ratio will help to determine the quantum numbers and the possible quark configuration as well.

V. SUMMARY

We have systematically evaluated the decay widths of the charmed baryons $\Lambda_c^*(2595)$, $\Lambda_c^*(2625)$, $\Lambda_c^*(2765)$, $\Lambda_c^*(2880)$, and $\Lambda_c^*(2940)$ into $\Sigma_c(2455)\pi$ and $\Sigma_c^*(2520)\pi$, as well as $\Sigma_c(2455)$ and $\Sigma_c^*(2520)$ into $\Lambda_c\pi$ within the

non-relativistic quark model. We have emphasized the usefulness of working in the baryon wave functions constructed to be consistent with heavy quark symmetry. This provides various selection rules associated with the pion emission between brown muck of the baryons. Our findings are as follows:

- For the low-lying $\Lambda_c^*(2595)$ and $\Lambda_c^*(2625)$ baryons the quark model descriptions as the λ-mode excitations with spin-0 diquark can explain the decay properties very well.
- The derivative coupling derived from the axial-vector interaction of πqq is essentially important to produce the experimental decay rate of $\Lambda_c^*(2595)$.
- Only one quark configuration $J_{\Lambda_c^*}(j)^P = 5/2(3)_2^+$ for $\Lambda_c^*(2880)$ among the possible five $5/2^+$ configurations can lead to the consistent result with the experimental data, while all other four configurations of $5/2^+$ cannot if the p-wave is properly considered. We note that the HQS does not necessarily lead to the small decay ratio of $\Gamma(\Sigma_c^*\pi)/(\Sigma_c\pi)$ for $5/2^+$. This fact calls an attention to the discussion based on the HQS [3, 30] which requires decays in only one partial wave.
- Having the above conclusion, we have discussed the possibility of $\Lambda_c^*(2940)$ being the HQS doublet partner of $\Lambda_c^*(2880)$ possessing $7/2(3)_2^+$. Here we emphasize that our results concerning the possible HQS doublet, $\Lambda_c^*(2880)$ and $\Lambda_c^*(2940)$, can be reached with jj coupling scheme which respects the heavy quark symmetry.
- The ratios of $\Gamma(\Sigma_c^*\pi)/\Gamma(\Sigma_c\pi)$ are considerably different for different quark configurations even if the baryon spin-parity is the same. This fact is particularly useful to know the structure of charmed baryons.

In this study, we have discussed the various constraints for the one-pion emission decays due to the selection rules associated with the brown muck spin j conservation. We have to keep it in mind, however, that there is still small breaking of heavy quark symmetry for charm quark. The study along this line will be left for future works.

In our discussions in the quark model, we have considered only the excitations of valence quarks. We expect that they provide a good description for low lying states. For higher excitations, however, there may be other modes such as pair creations of quark and anti-quark, gluon excitations and so on. The former can be taken into account in the quark model by couplings to mesons or by an unquenched configurations [48], and in effective hadron models by hadronic molecule configurations [49, 50]. The present systematic studies will help us to know where and how these configurations beyond the quark model ones show up which should be studied in the future J-PARC experiments.

ACKNOWLEDGMENT

The authors are grateful to K. Tanida and T. Yoshida for various discussions. This work is supported by Grants-in-Aid for Scientific Research (Grants No. JP26400275(C) for H. Nagahiro), (Grants No. JP15K17641 for S. Y.), (Grants No. JP26400273(C) for A. H.), (Grants No. JP16H02188(A) for H. Noumi) and (Grants No. JP25247036(A) for M. O., S. Y. and A. H.).

Appendix A: Harmonic oscillator wave functions

The radial functions $R_{n\ell}(\zeta)$ are given as,

$$R_{00}(\zeta) = \frac{2a_\zeta^{3/2}}{\pi^{1/4}} e^{-a_\zeta^2\zeta^2/2}, \tag{A1}$$

$$R_{01}(\zeta) = \left(\frac{8}{3}\right)^{1/2} \frac{a_\zeta^{5/2}}{\pi^{1/4}}\zeta, e^{-a_\zeta^2\zeta^2/2}, \tag{A2}$$

$$R_{02}(\zeta) = \left(\frac{16}{15}\right)^{1/2} \frac{a_\zeta^{7/2}}{\pi^{1/4}}\zeta^2, e^{-a_\zeta^2\zeta^2/2}, \tag{A3}$$

$$R_{10}(\zeta) = \frac{\sqrt{6}a_\zeta^{7/2}}{\pi^{1/4}} \left(1 - \frac{2}{3}a_\zeta^2\zeta^2\right) e^{-a_\zeta^2\zeta^2/2}, \tag{A4}$$

where

$$a_\zeta = \sqrt{m_\zeta \omega_\zeta}. \tag{A5}$$

The ζ is either λ or ρ. The reduced masses of m_λ and m_ρ are defined in Eq. (6).

Appendix B: Matrix elements

In this Appendix, we summerize the concrete forms of the helicity amplitudes A_h.

1. Ground state Σ_c decays

The amplitudes for the decays of $\Sigma_c^{(*)} \to \Lambda_c(1/2^+)\pi^-$ are given by

$$\begin{aligned} -iA_{1/2}^{\nabla\cdot\sigma} &= G\frac{\omega_\pi}{m}c\left(\frac{1}{2}q_\lambda + q_\rho\right)F(q), \\ iA_{1/2}^{q\cdot\sigma} &= -G\frac{q}{m}c\left(\frac{M}{2m+M}\omega_\pi - 2m\right)F(q), \end{aligned} \tag{B1}$$

where the coefficent c is given as

$$c = \begin{cases} -1/\sqrt{3} & \text{for } \Sigma_c(1/2^+)\ , \\ \sqrt{2/3} & \text{for } \Sigma_c^*(3/2^+)\ . \end{cases} \tag{B2}$$

The factor G denotes the coupling constant and the normalizations as,

$$G = \frac{g_A^q}{2f_\pi}\sqrt{2M_{\Lambda_c}}\sqrt{2M_{\Sigma_c^{(*)}}}\ , \tag{B3}$$

TABLE IX. Coefficients for the negative partiy Λ_c^* decays in Eq. (B5) .

λ-mode excitation ($\zeta=\lambda$)					
(n_λ,ℓ_λ) (n_ρ,ℓ_ρ)	$J_\Lambda(j)^P$	J_Σ^P	h	c_0	c_2
$(0,1)$, $(0,0)$	$1/2(1)^-$	$1/2^+$	$1/2$	$-\frac{1}{\sqrt{2}}$	$\frac{1}{3\sqrt{2}}$
		$3/2^+$	$1/2$	0	$-\frac{1}{3}$
	$3/2(1)^-$	$1/2^+$	$1/2$	0	$-\frac{1}{3}$
		$3/2^+$	$1/2$	$-\frac{1}{\sqrt{2}}$	$\frac{\sqrt{2}}{3}$
			$3/2$	$-\frac{1}{\sqrt{2}}$	0

ρ-mode exciation ($\zeta=\rho$)					
$(0,0)$, $(0,1)$	$1/2(0)^-$	$1/2^+$	$1/2$	0	0
		$3/2^+$	$1/2$	0	0
	$1/2(1)^-$	$1/2^+$	$1/2$	2	$-\frac{1}{3}$
		$3/2^+$	$1/2$	0	$-\frac{1}{3\sqrt{2}}$
	$3/2(1)^-$	$1/2^+$	$1/2$	0	$-\frac{1}{3\sqrt{2}}$
		$3/2^+$	$1/2$	2	$-\frac{1}{6}$
			$3/2$	2	$-\frac{1}{2}$
	$3/2(2)^-$	$1/2^+$	$1/2$	0	$\frac{1}{\sqrt{10}}$
		$3/2^+$	$1/2$	0	$\frac{1}{2\sqrt{5}}$
			$3/2$	0	$-\frac{1}{2\sqrt{5}}$
	$5/2(2)^-$	$1/2^+$	$1/2$	0	$\frac{1}{\sqrt{15}}$
		$3/2^+$	$1/2$	0	$\frac{1}{\sqrt{30}}$
			$3/2$	0	$\frac{1}{\sqrt{5}}$

and the function $F(q)$ denotes the gaussian form factor as

$$F(q) = e^{-q_\lambda^2/4a_\lambda^2} e^{-q_\rho^2/4a_\rho^2} \ . \tag{B4}$$

2. Negative parity $\Lambda_c^*(J^-)$ decays

The amplitudes for the decays of the negative parity excitations with p-wave of $\Lambda_c^*(J^-) \to \Sigma_c^{(*)}\pi$ are given by

$$\begin{aligned} -iA_h^{\nabla\cdot\sigma} &= iG\frac{\omega_\pi}{m}\ \left\{c_0 a_\zeta + c_2\left(\frac{1}{2}q_\lambda + q_\rho\right)\frac{q_\zeta}{a_\zeta}\right\}F(q)\ , \\ -iA_h^{q\cdot\sigma} &= iG\frac{q}{m}\left(\frac{M}{2m+M}\omega_\pi - 2m\right)(-1)c_2\frac{q_\zeta}{a_\zeta}F(q)\ , \end{aligned} \tag{B5}$$

where the coefficients c_0 and c_2 are summarized in Table IX. The subscript ζ is either λ or ρ, depending on the λ- or ρ-mode excitations.

3. Positive parity $\Lambda_c^*(J^+)$ decays

The amplitudes for the decays of the positive parity excitations with s-wave ($n_\zeta = 1$) or d-wave ($\ell_\zeta = 2$) of $\Lambda_c^*(J^-) \to \Sigma_c^{(*)}\pi$ are given by

TABLE X. Coefficients for the positive partiy $\Lambda_c^*(J^+)$ decays with s-wave ($n_\zeta = 1$) or d-wave ($\ell_\zeta = 2$) in Eq. (B6).

λ-mode excitation ($\zeta=\lambda$)					
(n_λ,ℓ_λ) (n_ρ,ℓ_ρ)	$J_{\Lambda_c^*}(j)^P$	$J_{\Sigma_c^{(*)}}$	h	c_1	c_3
$(1,0)$, $(0,0)$	$1/2(0)^+$	$1/2^+$	$1/2$	$\frac{1}{3\sqrt{2}}$	$-\frac{1}{6\sqrt{2}}$
		$3/2^+$	$1/2$	$-\frac{1}{3}$	$\frac{1}{6}$
$(0,2)$, $(0,0)$	$3/2(2)^+$	$1/2^+$	$1/2$	$\frac{1}{3}\sqrt{\frac{5}{2}}$	$-\frac{1}{3\sqrt{10}}$
		$3/2^+$	$1/2$	$-\frac{1}{6\sqrt{5}}$	$\frac{1}{3\sqrt{5}}$
			$3/2$	$-\frac{1}{2\sqrt{5}}$	0
	$5/2(2)^+$	$1/2^+$	$1/2$	0	$\frac{1}{2\sqrt{15}}$
		$3/2^+$	$1/2$	$\sqrt{\frac{3}{10}}$	$-\frac{1}{\sqrt{30}}$
			$3/2$	$\frac{1}{\sqrt{5}}$	0
ρ-mode excitation ($\zeta=\rho$)					
$(0,0)$, $(1,0)$	$1/2(0)^+$	$1/2^+$	$1/2$	$\frac{\sqrt{2}}{3}$	$-\frac{1}{6\sqrt{2}}$
		$3/2^+$	$1/2$	$-\frac{2}{3}$	$\frac{1}{6}$
$(0,0)$, $(0,2)$	$3/2(2)^+$	$1/2^+$	$1/2$	$\frac{\sqrt{10}}{3}$	$-\frac{1}{3\sqrt{10}}$
		$3/2^+$	$1/2$	$-\frac{1}{3\sqrt{5}}$	$\frac{1}{3\sqrt{5}}$
			$3/2$	$-\frac{1}{\sqrt{5}}$	0
	$5/2(2)^+$	$1/2^+$	$1/2$	0	$\frac{1}{2\sqrt{15}}$
		$3/2^+$	$1/2$	$\sqrt{\frac{6}{5}}$	$-\frac{1}{\sqrt{30}}$
			$3/2$	$\frac{2}{\sqrt{5}}$	0

$$\begin{aligned} -iA_h^{\nabla\cdot\sigma} &= G\frac{\omega_\pi}{m}\left\{c_1 q_\zeta + c_3\left(\frac{1}{2}q_\lambda + q_\rho\right)\frac{q_\zeta^2}{a_\zeta^2}\right\}F(q), \\ -iA_h^{q\cdot\sigma} &= G\frac{q}{m}\left(\frac{M}{2m+M}\omega_\pi - 2m\right)(-1)c_3\frac{q_\zeta^2}{a_\zeta^2}F(q). \end{aligned} \tag{B6}$$

where the coefficients c_1 and c_3 are summarized in Table X. The subscript ζ is either λ or ρ, depending on the λ- or ρ-mode excitations.

The amplitudes for the decays of the positive parity excitations with λ-ρ mixed excited states $(\ell_\lambda, \ell_\rho) = (1,1)$ of $\Lambda_c^*(J^-) \to \Sigma_c^{(*)}\pi$ are given by

TABLE XI. Coefficients for the positive partiy $\Lambda_c^*(J^+)$ decays with λ-ρ mixed excitations in Eq. (B7). ℓ denotes the total angular momentum defined by $\vec{\ell}=\vec{\ell}_\lambda+\vec{\ell}_\rho$.

λ-ρ mixed excitation						
(n_λ,ℓ_λ)	(n_ρ,ℓ_ρ)	$J_{\Lambda_c^*}(j)^P$	ℓ	$J^P_{\Sigma_c^{(*)}}$	h	$\tilde{c}_1$	$\tilde{c}_3$
$(0,1)$,	$(0,1)$	$5/2(2)^+$	2	$1/2^+$	1/2	0	$\frac{1}{3}\sqrt{\frac{1}{5}}$
				$3/2^+$	1/2	$-\frac{3}{2}\sqrt{\frac{1}{10}}$	$\frac{1}{3}\sqrt{\frac{1}{10}}$
				$3/2^+$	3/2	$-\frac{3}{2}\sqrt{\frac{1}{15}}$	$\frac{1}{\sqrt{15}}$
			1	$1/2^+$	1/2	0	0
				$3/2^+$	1/2	$-\frac{1}{2}\sqrt{\frac{3}{10}}$	0
				$3/2^+$	3/2	$-\frac{1}{2}\sqrt{\frac{1}{5}}$	0
		$5/2(3)^+$	2	$1/2^+$	1/2	0	$-\frac{2}{3}\sqrt{\frac{2}{35}}$
				$3/2^+$	1/2	0	$-\frac{2}{3}\sqrt{\frac{1}{35}}$
				$3/2^+$	3/2	0	$\sqrt{\frac{2}{105}}$
		$7/2(3)^+$	2	$1/2^+$	1/2	0	$-\sqrt{\frac{2}{105}}$
				$3/2^+$	1/2	0	$-\frac{1}{\sqrt{105}}$
				$3/2^+$	3/2	0	$-\frac{1}{\sqrt{21}}$

$$
\begin{aligned}
-iA_h^{\nabla\cdot\sigma} &= G\frac{\omega_\pi}{m}\left\{\tilde{c}_1\left((-1)^\ell 2a_\rho\frac{q_\lambda}{a_\lambda}+a_\lambda\frac{q_\rho}{a_\rho}\right)+\tilde{c}_3\frac{q_\lambda q_\rho}{a_\lambda a_\rho}\left(\frac{1}{2}q_\lambda+q_\rho\right)\right\}F(q),\\
-iA_h^{q\cdot\sigma} &= G\frac{q}{m}\left(\frac{M}{2m+M}\omega_\pi-2m\right)(-1)\tilde{c}_3\frac{q_\lambda q_\rho}{a_\lambda a_\rho}F(q),
\end{aligned}
\tag{B7}
$$

where ℓ denotes the total angular momentum $\vec{\ell}=\vec{\ell}_\lambda+\vec{\ell}_\rho$ and the coefficients $\tilde{c}_1$ and $\tilde{c}_3$ are summarized in Table XI.

Appendix C: Matrix elements in the heavy quark limit

In this appendix, we derive the matrix elements in the heavy quark limit to show how and when the geometric factor is separated, leading to the model independent relations [3]. Let us consider one pion emission of a heavy baryon containing one heavy quark Q and a pair of light quarks qq. Following the notation in this paper, let the initial baryon denoted by Λ_Q and the final one by Σ_Q. Then the spin and angular momentum couplings for the initial Λ_c and final $\Sigma_c\pi$ states are

$$
\begin{aligned}
|i\rangle &= |\Lambda_c\rangle = [j_{\Lambda_Q},s_Q]^{J_{\Lambda_c}M_{\Lambda_Q}},\\
|f\rangle &= |\Sigma_c\pi\rangle = [Y_L,[j_{\Sigma_Q},s_Q]^{J_{\Sigma_Q}}]^{J_fM_f},
\end{aligned}
\tag{C1}
$$

where J_{Λ_Q,Σ_Q} is the baryon spin, j_{Λ_Q,Σ_Q} the brown muck (light degrees of freedom) total spin, L the relative angular momentum of $\pi\Sigma_Q$, and J_f is the total spin $J_{\Sigma_Q}+L$. The decay probability is then computed as

$$
\Gamma\sim\sum_L|\langle f|\mathcal{L}_{int}|i\rangle|^2, \tag{C2}
$$

where $\mathcal{L}_{int}$ is the pion-quark interaction, and the sum over final state is taken over possible L's. For instance, for the decay of $5/2^+\to 3/2^+$, the angular momentum L can be both 1 (P-wave) and 3 (F-wave), while for the decay of $5/2^+\to 1/2^+$, only F-wave is possible.

In the literature, the model independent relation has been discussed for the ratio of the decays into $\Sigma_c^*(3/2^+)$ and into $\Sigma_c(1/2^+)$. In the heavy quark limit it can be obtained only for the decay into the same and single partial wave L. As we have discussed in IV D in detail, this is possible only in some limited cases where a selection rule due to the diquark transitions imposes an additional constraint. For a single L, after recouping the final state, we obtain the matrix element as follows,

$$
\begin{aligned}
&\langle[Y_L,[j_{\Sigma_Q},s_Q]^{J_{\Sigma_Q}}]^{J_fM_f}|\mathcal{L}_{int}|[j_{\Lambda_Q},s_Q]^{J_{\Lambda_Q}M_{\Lambda_Q}}\rangle\\
&=\sum_{j_f}\hat{J}_{\Sigma_Q}\hat{j}_f(-1)^{j_{\Sigma_Q}+S_Q+J_f+L}\begin{Bmatrix}J_{\Sigma_Q} & j_{\Sigma_Q} & s_Q\\ j_f & J_f & L\end{Bmatrix}\\
&\quad\langle[[Y_L,j_{\Sigma_Q}]^{j_f},s_Q]^{J_fM_f}|\mathcal{L}_{int}|[j_{\Lambda_Q},s_Q]^{J_{\Lambda_Q}M_{\Lambda_Q}}\rangle\ .
\end{aligned}
\tag{C3}
$$

Because the interaction $\mathcal{L}_{int}$ is active only for the light quarks, after the application of the Wigner-Eckart theorem, the matrix element in the third line can be factorized into the one of the light degrees of freedom, $\langle [Y_L, j_{\Sigma_Q}]^{j_f} || \mathcal{L}_{int} || j_{\Lambda_Q} \rangle$, and the trivial one of the heavy quark. If, furthermore, the brown muck configuration is uniquely determined, which is to fix j_f at a single value, the J_{Σ_Q} dependence is completely dictated by the 6-j symbol and the normalization $\hat{J}_{\Sigma_Q}$. This explains how and when the ratio in Eq. (75) can be determined in a model independent manner by the formula (C3).

[1] S. Weinberg, Phys. Rev. **130**, 776 (1963); **137**, B672 (1965).
[2] H. Nagahiro and A. Hosaka, Phys. Rev. **C90**, 065201 (2014), arXiv:1406.3684 [hep-ph].
[3] N. Isgur and M. B. Wise, Phys. Rev. Lett. **66**, 1130 (1991).
[4] M. Neubert, Phys. Rept. **245**, 259 (1994).
[5] S. Yasui and K. Sudoh, Phys. Rev. **D80**, 034008 (2009), arXiv:0906.1452 [hep-ph].
[6] Y. Yamaguchi, S. Ohkoda, S. Yasui, and A. Hosaka, Phys. Rev. **D85**, 054003 (2012), arXiv:1111.2691 [hep-ph].
[7] Y. Yamaguchi, S. Ohkoda, S. Yasui, and A. Hosaka, Phys. Rev. **D84**, 014032 (2011), arXiv:1105.0734 [hep-ph].
[8] Y. Yamaguchi, S. Yasui, and A. Hosaka, Nucl. Phys. **A927**, 110 (2014), arXiv:1309.4324 [nucl-th].
[9] C. Garcia-Recio, V. K. Magas, T. Mizutani, J. Nieves, A. Ramos, L. L. Salcedo, and L. Tolos, Phys. Rev. **D79**, 054004 (2009), arXiv:0807.2969 [hep-ph].
[10] D. Gamermann, C. Garcia-Recio, J. Nieves, L. L. Salcedo, and L. Tolos, Phys. Rev. **D81**, 094016 (2010), arXiv:1002.2763 [hep-ph].
[11] C. Garcia-Recio, J. Nieves, O. Romanets, L. L. Salcedo, and L. Tolos, Phys. Rev. **D87**, 034032 (2013), arXiv:1210.4755 [hep-ph].
[12] Y. Yamaguchi, S. Ohkoda, A. Hosaka, T. Hyodo, and S. Yasui, Phys. Rev. **D91**, 034034 (2015), arXiv:1402.5222 [hep-ph].
[13] Y.-R. Liu and M. Oka, Phys. Rev. **D85**, 014015 (2012), arXiv:1103.4624 [hep-ph].
[14] S. Maeda, M. Oka, A. Yokota, E. Hiyama, and Y.-R. Liu, PTEP **2016**, 023D02 (2016), arXiv:1509.02445 [nucl-th].
[15] S. Yasui, K. Sudoh, Y. Yamaguchi, S. Ohkoda, A. Hosaka, and T. Hyodo, Phys. Lett. **B727**, 185 (2013), arXiv:1304.5293 [hep-ph].
[16] S. Yasui and K. Sudoh, Phys. Rev. **C87**, 015202 (2013), arXiv:1207.3134 [hep-ph].
[17] S. Yasui and K. Sudoh, Phys. Rev. **C89**, 015201 (2014), arXiv:1308.0098 [hep-ph].
[18] S. Yasui, Phys. Rev. **D91**, 014031 (2015), arXiv:1408.3703 [hep-ph].
[19] D. Suenaga, B.-R. He, Y.-L. Ma, and M. Harada, Phys. Rev. **C89**, 068201 (2014), arXiv:1403.5140 [hep-ph].
[20] D. Suenaga, B.-R. He, Y.-L. Ma, and M. Harada, Phys. Rev. **D91**, 036001 (2015), arXiv:1412.2462 [hep-ph].
[21] D. Suenaga and M. Harada, Phys. Rev. **D93**, 076005 (2016), arXiv:1509.08578 [hep-ph].
[22] A. Hosaka, T. Hyodo, K. Sudoh, Y. Yamaguchi, and S. Yasui, (2016), arXiv:1606.08685 [hep-ph].
[23] T. Yoshida, E. Hiyama, A. Hosaka, M. Oka, and K. Sadato, Phys. Rev. **D92**, 114029 (2015), arXiv:1510.01067 [hep-ph].
[24] K. A. Olive *et al.* (Particle Data Group), Chin. Phys. **C38**, 090001 (2014).
[25] T.-M. Yan, H.-Y. Cheng, C.-Y. Cheung, G.-L. Lin, Y. C. Lin, and H.-L. Yu, Phys. Rev. **D46**, 1148 (1992), [Erratum: Phys. Rev.D55,5851(1997)].
[26] P. L. Cho, Phys. Lett. **B285**, 145 (1992), arXiv:hep-ph/9203225 [hep-ph].
[27] P. L. Cho, Phys. Rev. **D50**, 3295 (1994), arXiv:hep-ph/9401276 [hep-ph].
[28] J. L. Rosner, Phys. Rev. **D52**, 6461 (1995), arXiv:hep-ph/9508252 [hep-ph].
[29] C. Albertus, E. Hernandez, J. Nieves, and J. M. Verde-Velasco, Phys. Rev. **D72**, 094022 (2005), arXiv:hep-ph/0507256 [hep-ph].
[30] H.-Y. Cheng and C.-K. Chua, Phys. Rev. **D75**, 014006 (2007), arXiv:hep-ph/0610283 [hep-ph].
[31] X.-H. Zhong and Q. Zhao, Phys. Rev. **D77**, 074008 (2008), arXiv:0711.4645 [hep-ph].
[32] L. A. Copley, N. Isgur, and G. Karl, Phys. Rev. D **20**, 768 (1979).
[33] D. Pirjol and T.-M. Yan, Phys. Rev. **D56**, 5483 (1997), arXiv:hep-ph/9701291 [hep-ph].
[34] H. Albrecht *et al.* (ARGUS), Phys. Lett. **B317**, 227 (1993).
[35] K. W. Edwards *et al.* (CLEO), Phys. Rev. Lett. **74**, 3331 (1995).
[36] T. Aaltonen *et al.* (CDF), Phys. Rev. **D84**, 012003 (2011), arXiv:1105.5995 [hep-ex].
[37] P. L. Frabetti *et al.* (E687), Phys. Rev. Lett. **72**, 961 (1994).
[38] K. Abe *et al.* (Belle), *Proceedings of the 33rd International Conference on High Energy Physics (ICHEP '06)*, Phys. Rev. Lett. **98**, 262001 (2007), arXiv:hep-ex/0608043 [hep-ex].
[39] S. Weinberg, Phys. Rev. Lett. **65**, 1181 (1990).
[40] S. Weinberg, Phys. Rev. Lett. **67**, 3473 (1991).
[41] M. A. Morrison and G. A. Parker, Aust. J. Phys. , 465 (1987).
[42] A. Chodos, R. L. Jaffe, K. Johnson, and C. B. Thorn, Phys. Rev. **D10**, 2599 (1974).
[43] M. Artuso *et al.* (CLEO), Phys. Rev. Lett. **86**, 4479 (2001), arXiv:hep-ex/0010080 [hep-ex].
[44] H. Nagahiro and A. Hosaka, in progress.
[45] B. Aubert *et al.* (BaBar), Phys. Rev. Lett. **98**, 012001 (2007), arXiv:hep-ex/0603052 [hep-ex].
[46] S.-H. Kim, A. Hosaka, H.-C. Kim, H. Noumi, and K. Shirotori, Prog. Theor. Exp. Phys. **2014**, 103D01 (2014), arXiv:1405.3445 [hep-ph].
[47] H. Noumi *et al.*, http://www.j-parc.jp/researcher/Hadron/en/Proposal_e.html#1301 (2012), J-PARC E50 proposal.
[48] R. Bijker, J. Ferretti, and E. Santopinto, Phys. Rev. **C85**, 035204 (2012).

[49] T. Mizutani and A. Ramos, Phys. Rev. **C74**, 065201 (2006), arXiv:hep-ph/0607257 [hep-ph].

[50] J. Haidenbauer, G. Krein, U.-G. Meissner, and L. Tolos, Eur. Phys. J. **A47**, 18 (2011), arXiv:1008.3794 [nucl-th].